

CHALMERS



CHROMATIC DISPERSION COMPENSATION BY SIGNAL PREDISTORTION: LINEAR AND NONLINEAR FILTERING

SHAHAM SHARIFIAN

Communications Systems Group
Department of Signals and Systems
CHALMERS UNIVERSITY OF TECHNOLOGY
Göteborg, Sweden

EX026/2010

Abstract

Chromatic dispersion is one of the most significant impairments in long-distance fiber-optical communications. Electrical domain compensation of optical chromatic dispersion by signal predistortion using digital processing is investigated with two different approaches: using a linear digital FIR compensating filter and using a nonlinear filter based on a look-up table (LUT). The linear compensating system is simulated with quadrature phase shift keying (QPSK) and 16-quadrature amplitude modulation (16-QAM) schemes. In the 16-QAM system the maximum amplitude of the signal generated after the compensating filter can be large, so the maximum amplitude is calculated and is employed in compensating the cosine function of the Cartesian Mach-Zehnder modulator. The time and frequency domain implementation of the linear compensating filter are considered more carefully and the number of adjacent symbols which contribute to the intersymbol interference is calculated.

In [1] it has been shown that the LUT generated for compensating chromatic dispersion can be significantly compressed with the Hadamard transform. Nevertheless there are still some constraints in implementing such a system. These constraints, which are mainly memory constraints and processing time constraints, are introduced and some implementation details are discussed to avoid the memory constraints, e.g., the need for generating the large-size LUT before generating the compressed LUT. Removing this constraint allows us to go for longer input symbol sequences to the LUT. For example at the distance of 500 km in a 10 Gbaud/sec QPSK system, the chromatic dispersion can be completely compensated by taking 11 symbols as the input to the LUT. It is also shown that using at least a 4-bit digital-to-analog converter (DAC) in a QPSK system and a 5-bit DAC in a 16-QAM system does not lead to degradation of their performances.

The linear compensating filter can compensate any amount of dispersion in both modulation schemes with a reasonable number of filter taps. The LUT-based compensating system, with or without the Hadamard transform, has the same performance as the linear system, i.e., it can compensate CD completely, if the length of the input symbol stream to the LUT is chosen at least equal to the number of adjacent symbols which contribute to the intersymbol interference. For shorter input sequences to the LUT, we see degradation in the performance of the system, which can now be improved by the Hadamard transform, as previously shown in [1].

Keywords: Chromatic dispersion (CD), predistortion, electronic linear precompensation, nonlinear precompensation, look-up table, Hadamard transform, optical fiber communication, optical modulation formats, coherent detection, digital signal processing (DSP) .

Acknowledgments

Hereby I would like to thank my supervisor Prof. Erik Agrell for his support and insightful guidance. I also want to express my gratitude to the Ph.D. student of communication system group, Lotfollah Beygi, for always being available for various useful discussions. Thanks also to Dr. Pontus Johannisson and Prof. Magnus Karlsson at MC2 department for discussions about chromatic dispersion.

Göteborg, August 20, 2010

SHAHAM SHARIFIAN

NOTATION

AWGN	additive white Gaussian noise
CD	chromatic dispersion
DCF	dispersion compensating fibers
DDMZM	dual drive Mach-Zehnder modulator
DSP	digital signal processing
EDC	electronic dispersion compensation
EDFA	Erbium doped fiber amplifier
EPD	electronic predistortion
GVD	group velocity dispersion
ISI	intersymbol interference
LUT	look-up table
MMF	multimode fibers
OOK	on-off keying
PMD	polarization mode dispersion
QAM	quadrature amplitude modulation
RRC	root raised-cosine
SMF	single-mode fibers
SNR	signal-to-noise ratio

Contents

1	INTRODUCTION	1
2	FIBER-OPTIC COMMUNICATION SYSTEM	4
2.1	OPTICAL TRANSMITTER	4
2.1.1	THE MODULATOR	4
2.1.2	MODULATION SCHEMES	5
2.1.3	PULSE-SHAPING FILTERS	7
2.2	THE OPTICAL CHANNEL	8
2.2.1	CHROMATIC DISPERSION	9
2.2.2	TIME AND FREQUENCY RESPONSE	11
2.3	THE OPTICAL COHERENT RECEIVER AND DETECTION.....	11
2.4	LITERATURE STUDY ON CHROMATIC DISPERSION COMPENSATION	17
3	CHROMATIC DISPERSION COMPENSATION BY LINEAR FILTERING	19
3.1	SYSTEM MODEL	19
3.2	NUMBER OF FILTER TAPS	19
3.3	TIME-DOMAIN AND FREQUENCY-DOMAIN IMPLEMENTATIONS ..	21
3.4	EFFECT OF FILTERING ON THE AMPLITUDE	23
3.5	PERFORMANCE OF LINEAR PRECOMPENSATING METHOD	24
3.5.1	THE EFFECT OF D/A RESOLUTION ON THE PERFORMANCE	25
4	CHROMATIC DISPERSION COMPENSATION BY NONLINEAR FILTERING	28
4.1	THE TRANSMITTER SYSTEM MODEL	28
4.2	THE CONSTRAINTS AND THE SOLUTIONS	28
4.3	PERFORMANCE OF NONLINEAR PRECOMPENSATING METHOD ..	32
4.4	COMPARING WITH LINEAR COMPENSATION, PROS AND CONS ..	33

5 CONCLUSIONS

35

1 INTRODUCTION

A communication system is for transmitting information from one place to another by modulating an electromagnetic carrier wave. The carrier wave frequency varies from one system to another. Optical communication systems use high carrier frequencies (~ 100 THz) in the visible or ultraviolet region of the electromagnetic spectrum while wireless communication systems and microwave systems use lower carrier frequencies ($\sim 1-10$ GHz). Optical communication systems are sometimes called lightwave systems and when they employ optical fibers as the medium for transmitting information, they are called fiber-optic communication systems.

In a fiber-optic communication system different modulation formats can be used for modulating and sending pulses of light through an optical fiber. *On-off keying* (OOK) modulation was mostly used in digital lightwave systems until a few years ago because of its simplicity. As binary modulation formats have a low spectral efficiency, some advanced modulation schemes with higher spectral efficiency are more enticing to use. These multilevel modulations need coherent detection. Although coherent receivers increase complexity, they allow more advanced modulation techniques which leads to higher spectral efficiencies.

Compared to the bandwidth of radio communication systems (which is in range of \sim MHz), much higher bandwidth is available in fiber-optic systems (\sim THz) due to the much higher carrier frequency in fiber-optic systems than in wireless radio systems. This results in higher transmission data rates in fiber-optic communication systems (\sim Tb/s) compared to wireless radio communication systems (\sim Mb/s).

Supporting high data rates in long-distance transmissions, fiber-optic communication systems have revolutionized the telecommunication industry and they have been widely used in long-distance communications such as intercontinental, transatlantic and transpacific communications. Today most of the copper wires in core of global telecommunication infrastructure are replaced by optical fibers due to much lower attenuation and interference.

An optical fiber consists of three parts: a core, a cladding, and a buffer (an outer coating to protect cladding). The cladding and the core are usually made from high quality silica glass or sometimes from plastic. The cladding has a lower refractive index, so the light is guided along the core by the total internal refraction method. Multimode fibers (MMF) and single-mode fibers (SMF) are two main types of optical fibers used in fiber-optic communications. SMF has a smaller core radius (< 10 micrometers) than MMF (≥ 50 micrometers). SMF interconnectors and components are usually more expensive but the performance of this type of link is higher than MMF link. MMF links have higher attenuation and because of introducing multimode distortion, they often limit the bandwidth and length of the link. In this thesis we consider SMF as the transmission medium. In such a medium the following impairments limit the performance of the system [2, pp. 39–64]:

- Fiber losses limit the transmission distance.
- Dispersion limits the bit rate due to pulse broadening.
- Nonlinear effects limit the system performance due to distortion of the signal.

Fiber losses are because of material absorption, scattering, or waveguide imperfections and they attenuate the average power reaching the receiver. To compensate this attenuation optical amplifiers are used periodically. In long-haul transmission systems, the spacing between repeaters is mainly determined by the amount of fiber loss. The bandwidth that can be transmitted through the optical-fiber is considerably limited by chromatic dispersion. There are two kinds of dispersion: chromatic dispersion (CD) and polarization mode dispersion (PMD). The refractive index of the fiber is frequency dependent, so different frequency components travel at different speeds and they arrive at different times at the output end which leads to pulse broadening and intersymbol interference (ISI). This phenomenon is known as chromatic dispersion. The components that are orthogonally polarized also travel at different speeds due to manufacturing defects, stress, vibration or other imperfections which causes polarization mode dispersion. PMD can degrade system performance considerable especially for old fibers and at high data rates. Major nonlinear effects in optical fibers are stimulated Raman scattering, stimulated Brillouin scattering, self-phase modulation (SPM), cross-phase modulation, and four-wave mixing.

In this thesis we do not consider nonlinear effects and we just deal with chromatic dispersion which is a linear phenomenon. Chromatic dispersion limits the bandwidth and thus the transmission data rate because of pulse spreading. The chromatic dispersion can be compensated in both electrical and optical domains. The main goal of this thesis is designing linear and nonlinear electronic dispersion compensator systems using a finite impulse response (FIR) filter and a look-up table (LUT) respectively and analyzing and comparing the two systems. Some implementation consideration on the linear system is also discussed. Chapter 1 introduces the fiber-optic communication system, the impairments that exist in such a system and the main goal of the thesis. The fiber-optic communication system model is described in Chapter 2, where the optical transmitter, channel, and receiver are reviewed. Toward the end of this chapter different modulation formats and pulse-shaping filters are introduced and dispersion is studied more carefully. The chapter ends with a literature study on different techniques that has been used to compensate fiber impairments, particularly fiber dispersion. The linear system design for compensating CD is explained in Chapter 3. In this chapter, we consider a real-time linear finite impulse response (FIR) filter to compensate CD. This filter can be implemented in both time and frequency domain. A lower bound on the number of filter taps required for compensating chromatic dispersion as a function of sampling frequency and pulse-shaping filter bandwidth is derived. In addition, an expression for the number of adjacent symbols which contribute to the ISI is given and the maximum amplitude generated after the FIR compensator filter is calculated and used in compensating the modulator effect. The performance of the system is shown and the

effect of digital-to-analog resolution on the performance is investigated. The nonlinear filtering design is discussed in Chapter 4. In [1] it has been shown that the LUT generated for compensating chromatic dispersion can be significantly compressed with the Hadamard transform. Nevertheless there are still some constraints, such as memory constraints, in implementing such a system. In this chapter some implementation details are discussed to avoid the memory constraints such as the need for generating the large-size LUT before generating the compressed LUT. Moreover, at the end of this chapter the linear and nonlinear implemented systems are compared in sense of performance, memory requirement and computational complexity. Finally this thesis work is concluded with some conclusions in Chapter 5.

2 FIBER-OPTIC COMMUNICATION SYSTEM

2.1 OPTICAL TRANSMITTER

Common optical sources in fiber-optic communication systems are semiconductor optical sources such as light-emitting diodes (LEDs) or semiconductor lasers which are also known as laser diodes or injection lasers. The electrical input signal must be converted to an optical signal before launching it into the optical fiber. This is done by modulating the optical source and can be accomplished in two ways: direct modulation or using an external optical modulator. In direct modulation, the light source's driving current is directly modulated by the electrical drive signals. Although this method is less complex, it is not achievable in high-speed transmissions due to its large spectral width. So in applications with high bit rates, an external modulator is applied to modulate the light carrier by the electrical data signal.

2.1.1 THE MODULATOR

An external modulator that has been widely used is the dual drive Mach-Zehnder modulator (DDMZM). As shown in Figure 2.1, the DDMZM divides the incoming optical signal into two signals. Each wave propagates through one arm of the DDMZM. Applying voltage to each arm results in a phase shift in the optical signal. Then the phase shifted waves are added to form the modulated optical signal.

The transfer function of DDMZM is [3]:

$$\begin{aligned} E_{\text{out}}(t) &= \frac{1}{2} \left(E_{\text{in}}(t) e^{j\pi \frac{V_1(t)}{V_\pi}} \right) + \frac{1}{2} \left(E_{\text{in}}(t) e^{j\pi \frac{V_2(t)}{V_\pi}} \right) \\ &= E_{\text{in}}(t) \cos \left(\frac{\pi}{2} \cdot \frac{V_1(t) - V_2(t)}{V_\pi} \right) e^{j\pi \frac{V_1(t) + V_2(t)}{2V_\pi}}, \end{aligned} \quad (2.1)$$

where E_{in} is the input optical signal to the modulator, E_{out} is the output optical

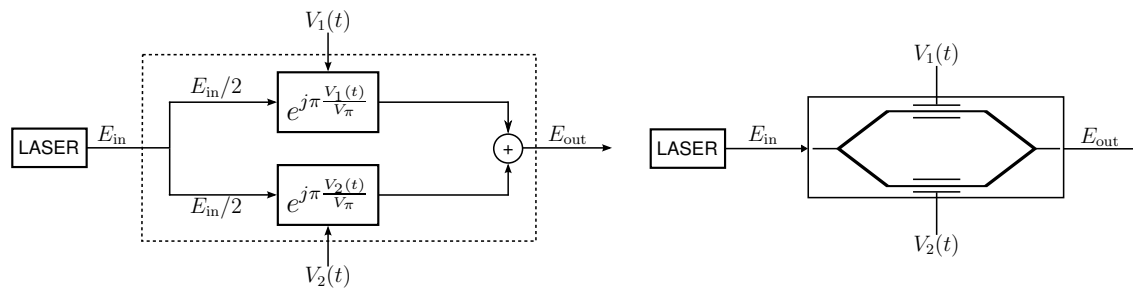


Figure 2.1: Block diagram of dual drive Mach-Zehnder [1].

signal from the modulator, $V_1(t)$ and $V_2(t)$ are the drive signals to the two arms of DDMZM and V_π is a reference voltage. V_π is typically around 4 volts.

It can be seen from above equation that DDMZM can modulate both amplitude and phase of the optical signal. If the same drive signal is applied to both arms, *i.e.*, when $V_1(t) = V_2(t)$, the DDMZM operates as a phase modulator (PM) while when $V_1(t) = -V_2(t)$ the DDMZM acts as an amplitude modulator (AM) and the transfer function is simplified to

$$E_{\text{out}}(t) = E_{\text{in}}(t) \cos\left(\frac{\pi V_1(t)}{V_\pi}\right). \quad (2.2)$$

2.1.2 MODULATION SCHEMES

The optical carrier before modulation has the form [2, p. 14] :

$$\mathbf{E}_{\text{in}}(t) = \hat{\mathbf{e}} A_c \cos(\omega_c t + \varphi), \quad (2.3)$$

where $\mathbf{E}_{\text{in}}(t)$ is the electric field vector, $\hat{\mathbf{e}}$ is the polarization unit vector (if $\hat{\mathbf{e}}$ is a scalar unit it results in the scalar $E_{\text{in}}(t)$), A_c is the amplitude, ω_c is the carrier frequency and φ is the carrier phase. So different modulation formats can be used as follows:

- Amplitude-shift keying (ASK), in which A_c is modulated
- Frequency-shift keying (FSK), in which ω_c is modulated
- Phase-shift keying (PSK), in which φ is modulated
- Polarization-shift keying (PoSK), in which information are encoded in the polarization state $\hat{\mathbf{e}}$ of each bit.

The PoSK modulation is not practical for optical fibers. Most digital lightwave systems use ASK which is also known as intensity modulation. Multilevel intensity modulation results in a significant increase in required SNR. The simplest way to apply intensity modulation is changing the signal intensity between zero and another level which is often called *on-off keying* (OOK). But as binary modulation formats have a low spectral efficiency, some advanced modulations with higher spectral efficiency are considered recently. Using coherent detection with multilevel modulation formats increases complexity but leads to higher spectral efficiency. QPSK and Differential QPSK (DQPSK) have attracted more attention among the advanced modulation formats as they have reasonable complexity and a higher tolerance to fiber chromatic dispersion, polarization mode dispersion and nonlinearities [3].

M-ary quadrature amplitude modulation (QAM) is a widely used modulation format in communication systems as it utilizes the signal space more than other modulation formats when the number of symbols increases. The optical QAM format can be

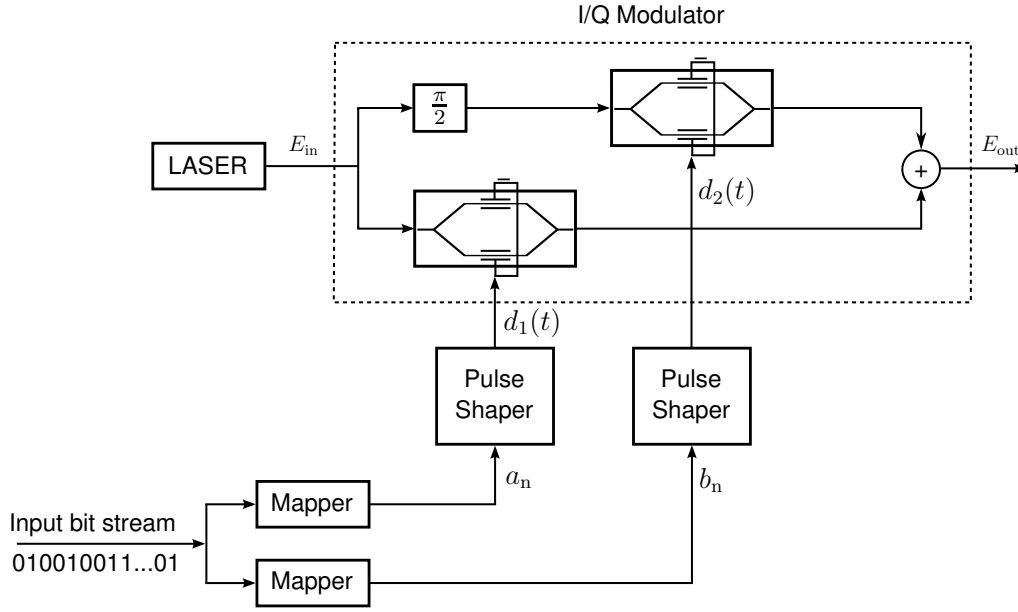


Figure 2.2: Block diagram of optical I/Q modulator [3].

generated with an I/Q modulator structure shown in Figure 2.2. The I/Q modulator can be generated by using two MZMs, each acts as an amplitude modulator. Considering Equations (2.2) and (2.3), the transfer function of the I/Q modulator can be written as

$$\begin{aligned}
 E_{\text{out}}(t) &= \frac{A_c}{2} \cos\left(\frac{\pi}{V_\pi} d_1(t)\right) \cos(\omega_c t + \varphi) - \frac{A_c}{2} \cos\left(\frac{\pi}{V_\pi} d_2(t)\right) \sin(\omega_c t + \varphi) \quad (2.4) \\
 &= \frac{A_c}{2} \cos\left[\frac{\pi}{V_\pi} \sum_n (a_n p(t - nT_s))\right] \cos(\omega_c t + \varphi) - \frac{A_c}{2} \cos\left[\frac{\pi}{V_\pi} \sum_n (b_n p(t - nT_s))\right] \sin(\omega_c t + \varphi)
 \end{aligned}$$

where $d_1(t)$ and $d_2(t)$ are the drive signals to the two MZMs, a_n and b_n are the mappers outputs, $p(t)$ is the pulse-shaping filter discussed in the next section, and T_s is the symbol duration.

This type of modulator is also called the Cartesian MZM. The advantage of Cartesian MZM, compared with dual-drive MZM, is that linear impairments in the fiber, such as dispersion, can be compensated by deploying only linear filtering (Chapter 3), while with the dual-drive MZM nonlinear filtering is required. Another advantage of Cartesian MZM is introducing less errors because of limited resolution of DSP [4]. However they are more expensive and complex. They introduce higher optical loss and they typically need more drive power to minimize loss [5]. In this thesis we only apply Cartesian MZMs (i.e. I/Q modulators) and we consider different modulation schemes such as OOK, BPSK, QPSK (which is identical to 4-QAM), and 16-QAM. Using multi level modulation formats such as 16-QAM instead of conventional binary modulations can significantly increase bandwidth efficiency.

2.1.3 PULSE-SHAPING FILTERS

The waveform of the transmitted pulses is usually changed before sending it into the channel. This process is done to limit the effective bandwidth of the transmission, and have a better control over the intersymbol interference caused by the channel. So the pulse-shaping filter determines the spectrum of the transmission. Pulse-shaping filters need to satisfy certain criteria so that the filter itself does not introduce ISI. Common criteria for evaluating filters are Nyquist ISI criterion and orthogonal pulse criterion [6, pp. 13–29]. The Nyquist pulses are appropriate for sampling receivers whereas the orthogonal pulses are usually used as pulse-shaping filters in the transmitter and as matched filters in the receiver. Some common pulse-shaping filters are as follows:

- Raised-cosine (RC in the time domain) filter: The RC in time domain has infinitely wide bandwidth, therefore its practical applications are limited to the communication channels that have some extra bandwidth. The RC in time domain is a Nyquist pulse and has the following equation:

$$p(t) = \begin{cases} 1, & |t| \leq \frac{T_s}{2} (1 - \alpha) \\ \cos^2 \left[\frac{\pi}{4} \frac{2|t| - T_s(1 - \alpha)}{\alpha T_s} \right], & \frac{T_s}{2} (1 - \alpha) < |t| \leq \frac{T_s}{2} (1 + \alpha) \\ 0, & |t| > \frac{T_s}{2} (1 + \alpha) \end{cases} \quad (2.5)$$

where T_s is the symbol duration, α is the roll-off factor, and $0 < \alpha < 1$.

- Boxcar filter: Such signals are the simplest possible waveforms as they are naturally created by digital electronics. The boxcar filter, like the RC in time domain filter, is a Nyquist pulse and has an infinitely wide bandwidth. In optical fibers or even in twisted pair cables, where enough bandwidth is available, it makes sense to use such a simple pulse to reduce the limitation that electronic equipments cause for data transmission rate. But in general, choosing a wide-band pulse-shaping filter is not a wise choice since the low-pass filter in the receiver side cuts the signal bandwidth which leads to an ISI in the system.
- Root raised-cosine (RRC) filter: This filter, together with a matched filter at the receiver side, is widely used in practical implementations. The roll-off factor parameter, α , determines the excess bandwidth. Smaller values of α lead to less spectral efficiency and less complex filters. The RRC pulse is an

orthogonal pulse and has the following time response:

$$p(t) = \begin{cases} \frac{1}{\sqrt{T_s}} \left(1 - \alpha + \frac{4\alpha}{\pi}\right), & t = 0 \\ \frac{\alpha}{\sqrt{2T_s}} \left[\left(1 + \frac{2}{\pi}\right) \sin\left(\frac{\pi}{4\alpha}\right) + \left(1 - \frac{2}{\pi}\right) \cos\left(\frac{\pi}{4\alpha}\right) \right], & t = \pm \frac{T_s}{4\alpha} \\ \frac{1}{\sqrt{T_s}} \frac{\sin\left[\pi(1-\alpha)\frac{t}{T_s}\right] + \frac{4\alpha}{T_s} t \cos\left[\pi(1+\alpha)\frac{t}{T_s}\right]}{\frac{\pi}{T_s} t \left[1 - \left(4\alpha\frac{t}{T_s}\right)^2\right]}, & \text{otherwise} \end{cases} \quad (2.6)$$

- Gaussian filter: The impulse response of a Gaussian filter is a Gaussian function given by

$$p(t) = \frac{1}{\sigma\sqrt{2\pi}} e^{-\frac{t^2}{2\sigma^2}}, \quad (2.7)$$

where σ is the standard deviation. The Fourier transform of the Gaussian pulse is a Gaussian function. The Gaussian pulse is neither a Nyquist pulse nor an orthogonal pulse, but if we consider that a high proportion of the pulse energy is included in one symbol time, this pulse can be approximately considered as both Nyquist and orthogonal pulses for sufficiently small σ .

- E33 pulse [7]: This kind of pulse is limited to one symbol time, T_s , thus it is both a Nyquist and an orthogonal pulse. The transfer function is given by

$$p(t) = \begin{cases} \frac{1}{\sqrt{E_{33}}} \sin\left(\frac{\pi}{2} \left[1 + \sin\left(\frac{\pi t}{T_s}\right)\right]\right), & -\frac{T_s}{2} \leq |t| \leq \frac{T_s}{2} \\ 0, & \text{otherwise} \end{cases} \quad (2.8)$$

where E_{33} is the energy of the pulse.

In this thesis different pulse-shaping filters such as RRC filter, Gaussian filter, RC in the time domain filter, and E33 filter are considered. Figure 2.3 shows the time-domain representation of these filters with unit energy, and their corresponding frequency responses are also shown in Figure 2.4.

2.2 THE OPTICAL CHANNEL

As briefly discussed previously, using fiber as the transmission medium in fiber-optic communication systems introduces different impairments such as fiber losses, dispersion, and nonlinear effects compared to wireless channels. This report only focuses on dispersion in SMFs. Fiber dispersion, which is a linear phenomenon, is studied more carefully below.

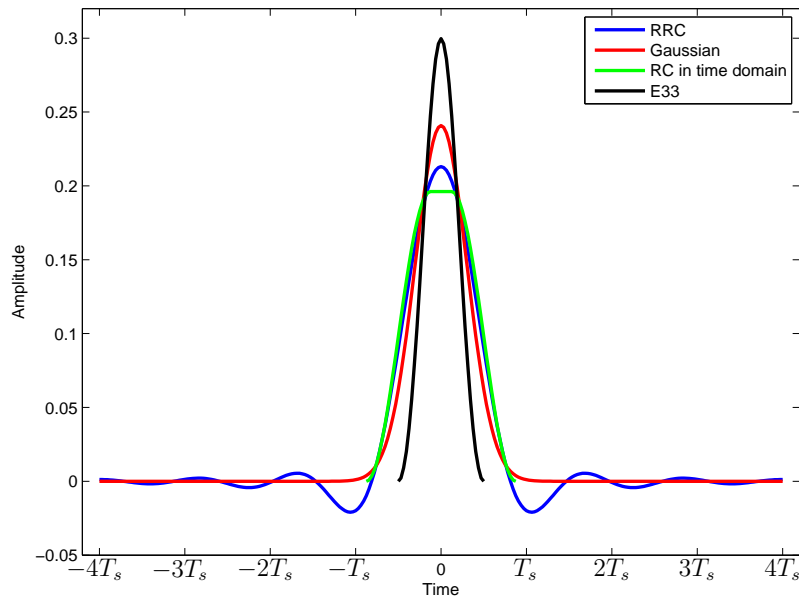


Figure 2.3: Time response of different unit-energy pulse-shaping filters: (RRC pulse with $\alpha = 0.75$, Gaussian pulse with 80% of its energy contained in the symbol time, RC in time domain with $\alpha = 0.75$, and E33 pulse).

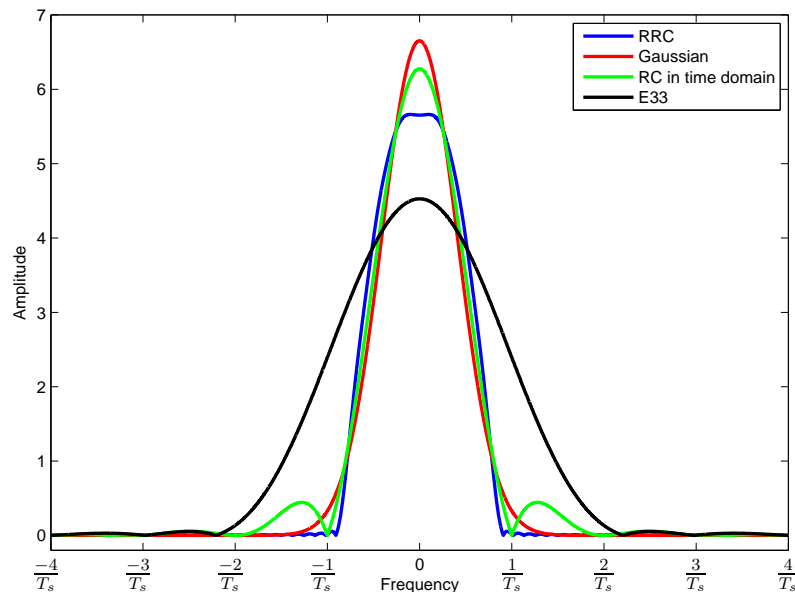


Figure 2.4: Frequency response of different unit-energy pulse-shaping filters: (RRC pulse with $\alpha = 0.75$, Gaussian pulse with 80% of its energy contained in the symbol time, RC in time domain with $\alpha = 0.75$, and E33 pulse).

2.2.1 CHROMATIC DISPERSION

Optical fibers introduce two kinds of dispersion, intermodal and intramodal dispersion, each of them leads to pulse broadening inside the fiber. Intermodal or modal dispersion happens because the signal propagation speed is not the same for all

modes of fiber. This kind of dispersion only occurs in MMFs and that is why most fiber-optic communication systems do not use MMFs. Intramodal dispersion, which is known as group velocity dispersion (GVD), chromatic dispersion, or simply fiber dispersion, exists in both SMFs and MMFs. There are two kinds of dispersion that contribute in intramodal dispersion, namely material dispersion and waveguide dispersion. Material dispersion happens because different wavelengths that enter the fiber at the same time, travel at different velocities in the fiber and exit the fiber at different times. This is because the refractive index of the fiber core is frequency-dependant. Therefore material dispersion depends on the source spectral width and is less at longer wavelengths. The reason for waveguide dispersion is that the propagation constant, β , is a function of fiber core size and wavelength. Moreover the refractive indexes of the core and the cladding are different, so light propagates differently in them.

Chromatic dispersion becomes more serious at higher bit rates (> 10 Gb/s) and highly degrades the system efficiency in the way that it limits the information capacity and transmission distance in the fiber-optic channel due to pulse broadening. As mentioned before, pulse broadening stems from frequency dependence of β . It is useful to write the Taylor-expansion of propagation constant, $\beta(\omega)$, around the carrier frequency ω_c :

$$\beta(\omega) = \beta(\omega_c) + \beta'(\omega_c)(\omega - \omega_c) + \frac{1}{2!}\beta''(\omega_c)(\omega - \omega_c)^2 + \frac{1}{3!}\beta'''(\omega_c)(\omega - \omega_c)^3 + \dots \quad (2.9)$$

$$= \beta_0 + \beta_1(\omega - \omega_c) + \frac{1}{2!}\beta_2(\omega - \omega_c)^2 + \frac{1}{3!}\beta_3(\omega - \omega_c)^3 + \dots$$

where $\beta_m = \frac{\partial^m \beta}{\partial \omega^m} |_{\omega=\omega_c}$ and the derivatives are taken with respect to angular frequency ω . Considering the above equation, we have the following definitions and relations [2, pp. 40–47]:

$$\text{Wave number: } \beta_0 = \frac{\partial \beta}{\partial \omega} |_{\omega=\omega_c} = \frac{2\pi}{\lambda} \quad (2.10)$$

$$\text{GVD parameter: } \beta_2 = \frac{\partial^2 \beta}{\partial \omega^2} |_{\omega=\omega_c} \quad (2.11)$$

$$\text{Phase velocity: } v_p = \frac{c}{n} = \frac{\omega}{\beta_0} \quad (2.12)$$

$$\text{Group velocity: } v_g = \left(\frac{\partial \beta}{\partial \omega} \right)^{-1} \quad (2.13)$$

$$\text{Dispersion parameter: } D = \frac{\partial}{\partial \lambda} \left(\frac{1}{v_g} \right) = -\frac{2\pi c}{\lambda^2} \beta_2 \quad (2.14)$$

$$\text{Second-order dispersion parameter: } S = \left(\frac{2\pi c}{\lambda^2} \right)^2 \beta_3 + \left(\frac{4\pi c}{\lambda^3} \right) \beta_2 \quad (2.15)$$

where λ is the operating wavelength, n is the refractive index, and c is the free-space speed of light. The dispersion parameter, D , is often known for a fiber and its typical value is 17 ps/(km.nm) for a SMF. The GVD parameter, β_2 , is usually expressed in units of ps²/km.

2.2.2 TIME AND FREQUENCY RESPONSE

If we ignore polarization mode dispersion and nonlinearities of the fiber-optic channel and only consider the chromatic dispersion, the channel can be modeled as a linear channel. The transfer function of a fiber of length d is given by

$$H(\omega) = e^{-j\beta(\omega)d}. \quad (2.16)$$

Considering Equation (2.9), the constant term and the linear term do not cause dispersion. It can also be shown that the third and higher order terms have a small role in dispersion compared with the second order term [8]. Thus, by replacing Eq.(2.9) in Eq.(2.16) and setting $\omega_c = 0$, the baseband transfer function of CD can be approximately written as

$$H(\omega) = e^{-j\frac{\beta_2 d}{2}\omega^2} = e^{j\frac{D\lambda^2 d}{4\pi c}\omega^2}. \quad (2.17)$$

It can be seen that CD is an all-pass filter with gain one. Taking the inverse Fourier transform of equation above gives the impulse response of CD as

$$h(t) = \sqrt{\frac{1}{j2\pi\beta_2 d}} e^{j\frac{t^2}{2\beta_2 d}} = \sqrt{\frac{j c}{D\lambda^2 d}} e^{-j\frac{\pi c}{D\lambda^2 d}t^2}. \quad (2.18)$$

So the impulse response of the dispersive fiber is linear time-invariant, infinite in time, and noncausal. The real and imaginary part of this chirp are shown in Figure 2.5.

The constellation diagram of the I/Q modulator (Fig. 2.2), employing different pulse-shaping filters, with QPSK and 16-QAM modulation formats, and the effect of CD on the constellation diagram at different distances are shown in Figures 2.6–2.8. As CD greatly depends on the previous and future transitions, the effect of CD varies by changing the transition pattern. These figures also show that the CD effect is more severe at larger fiber lengths.

2.3 THE OPTICAL COHERENT RECEIVER AND DETECTION

The optical receiver goal is to recover the source data that is transmitted through the lightwave system. To do that, first the optical signal should be converted into an electrical signal. This task can be done via using any type of photodetectors

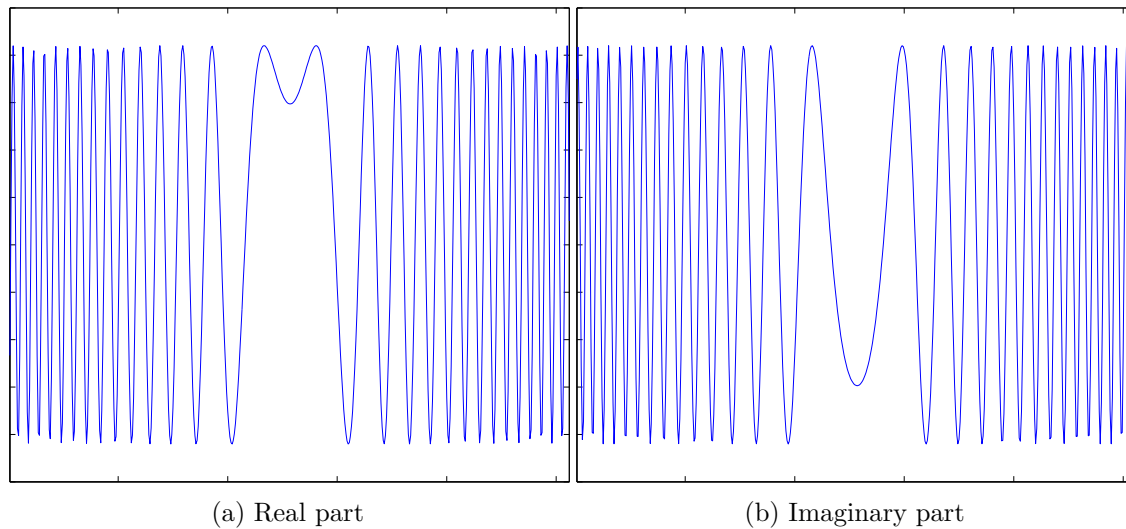


Figure 2.5: Real and imaginary part of chromatic dispersion in time domain.

such as photodiodes. A noncoherent receiver with direct detection only detects the intensity (amplitude) of the signal. This type of receiver is very simple as it does not need any phase or frequency information. But as previously mentioned in Chapter 1 and Section 2.1.1, binary modulation formats, such as OOK, with direct detection have low spectral efficiencies. Multilevel intensity modulations with direct detection also result in a significant increase in required SNR. So some advanced modulation schemes with higher spectral efficiencies, such as M-PSK and M-QAM, are considered recently. These multilevel modulations need coherent detection. In a coherent receiver the carrier phase is recovered by receiver circuitry and the phase information is used in demodulating the received signal. Although coherent modulation increases the spectral efficiency and usually requires less power than noncoherent modulation to achieve a given error rate, it also increases the complexity of the receiver.

Figure 2.9 shows the block diagram and the equivalent mathematical model of a homodyne coherent I/Q demodulator which consists of an optical amplifier, an optical bandpass filter, optical hybrids, photodiodes, electrical lowpass filters, and sampling and detection units [3].

Photodiodes perform squaring operation which causes losing the phase information. In a coherent detection system the phase information is recovered by mixing the incoming signal with a continuous-wave reference signal from a local oscillator (LO). This is done in the optical hybrids which are key components for coherent receivers. By employing linear interconnected dividers and combiners and performing different additions of the reference signal, $\pi/2$ phase shifted reference signal, and the incoming signal, the optical hybrids deliver the inphase and quadrature signals. Optical hybrids can be used for either homodyne or heterodyne detection. In a homodyne detection the local oscillator signal is synchronized in frequency to the carrier of the incoming signal while in a heterodyne detection there is a difference between the

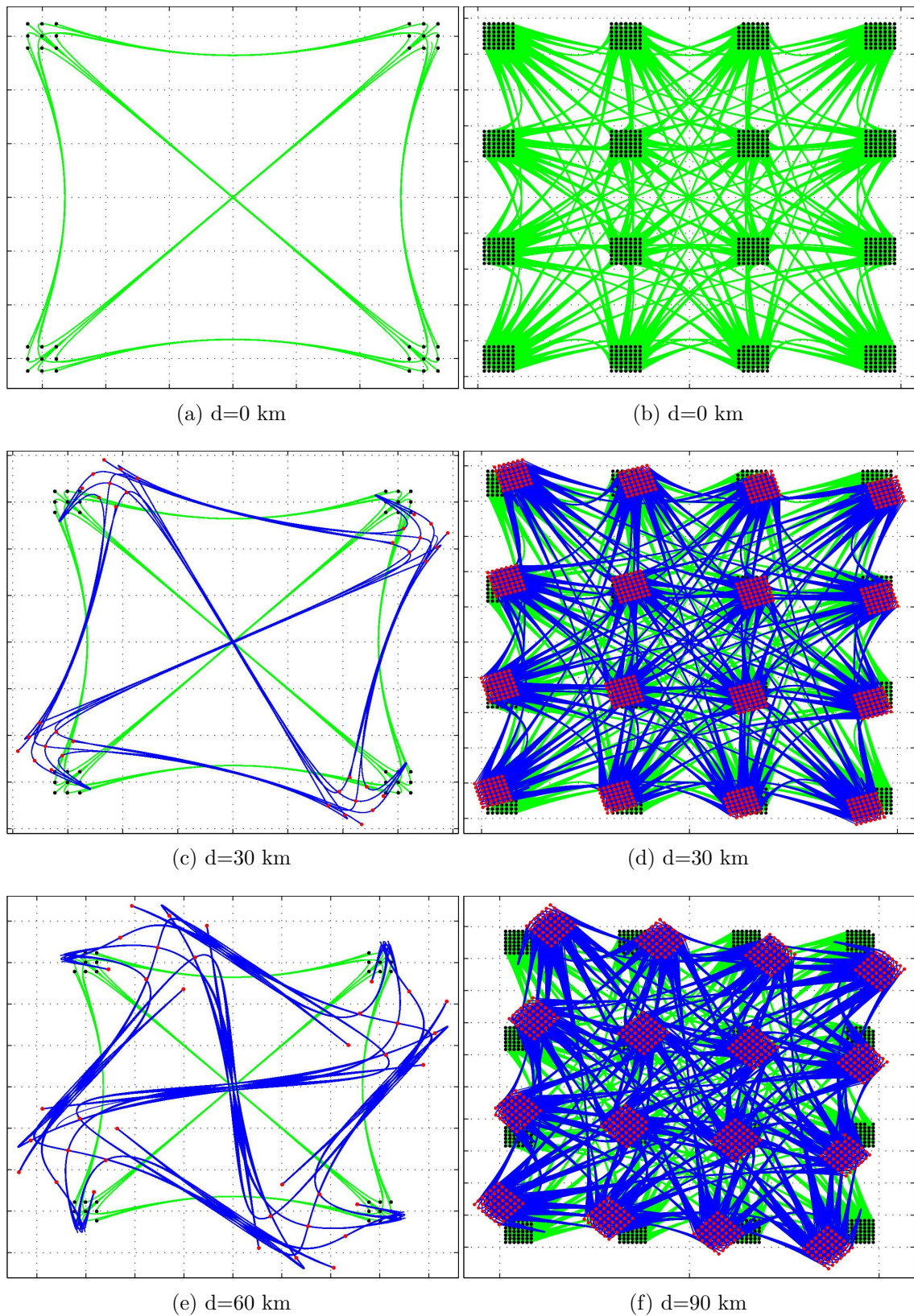


Figure 2.6: Effect of CD on the QPSK (left) and 16-QAM (right) constellation diagrams using Gaussian pulse-shaping filter (80% of the pulse energy contained in a symbol time). $\beta_2 = 22 \text{ ps}^2/\text{km}$.

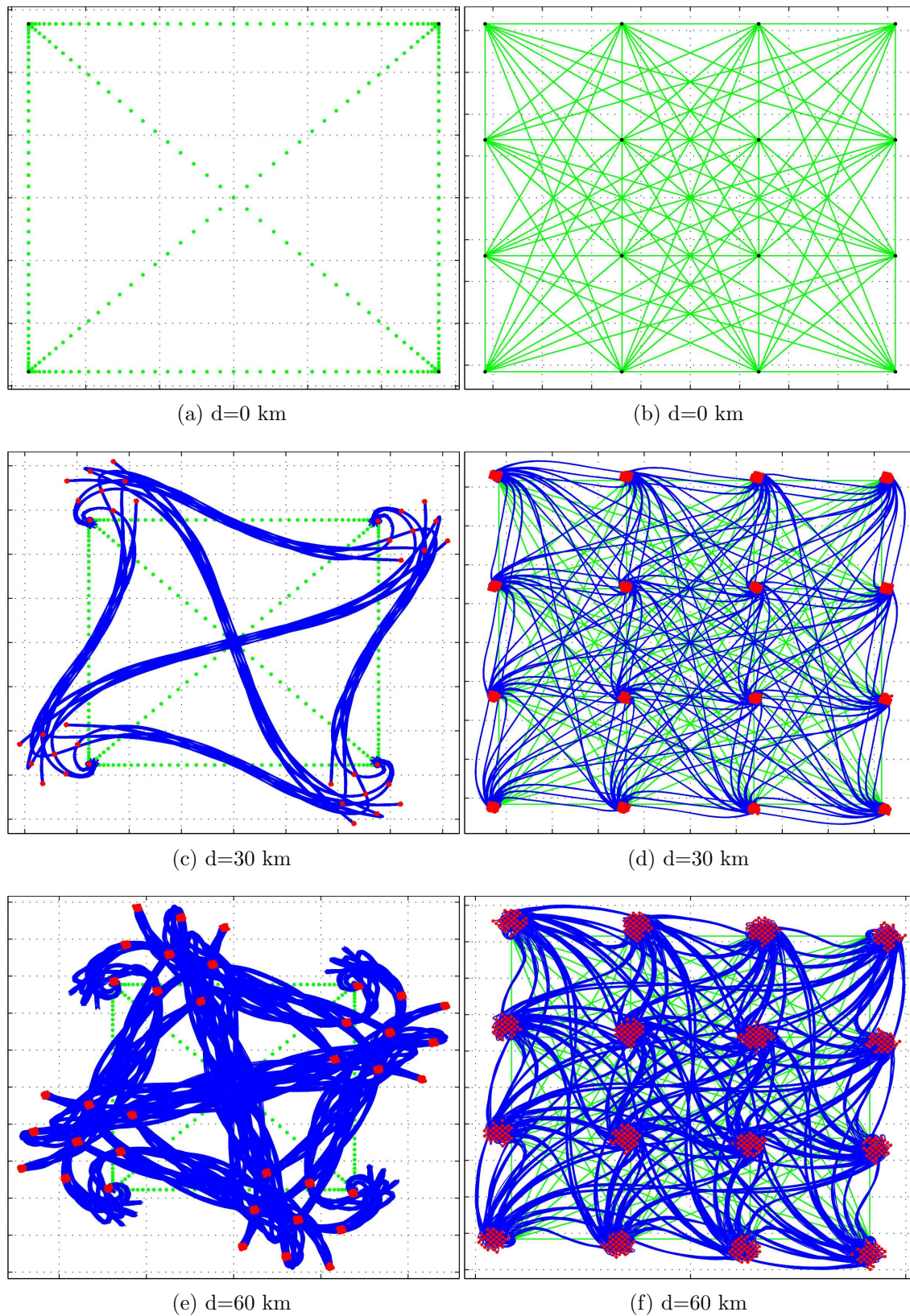


Figure 2.7: Effect of CD on the QPSK (left) and 16-QAM (right) constellation diagrams using RC pulse-shaping filter ($\alpha = 0.75$). $\beta_2 = 22$ ps²/km.

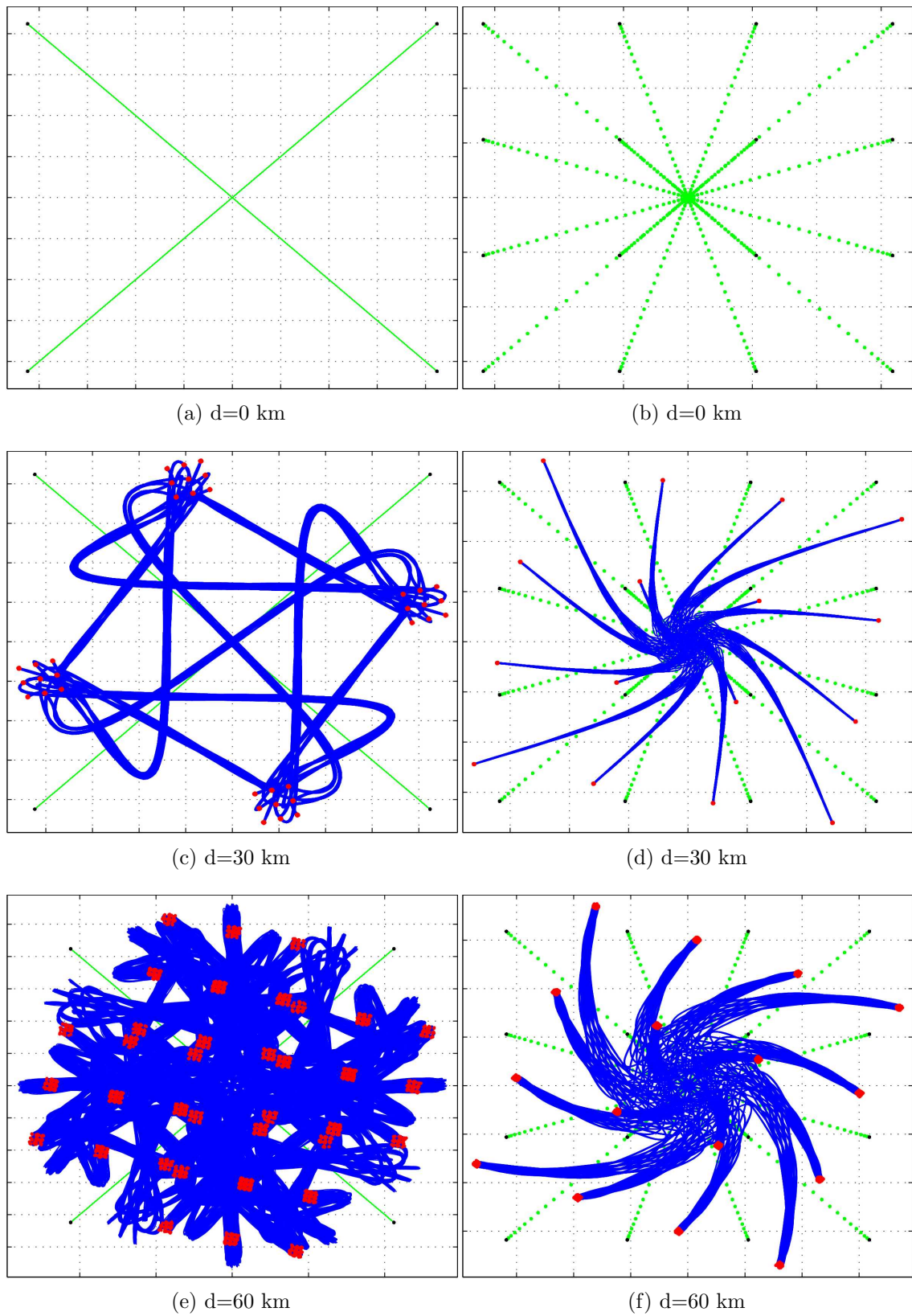
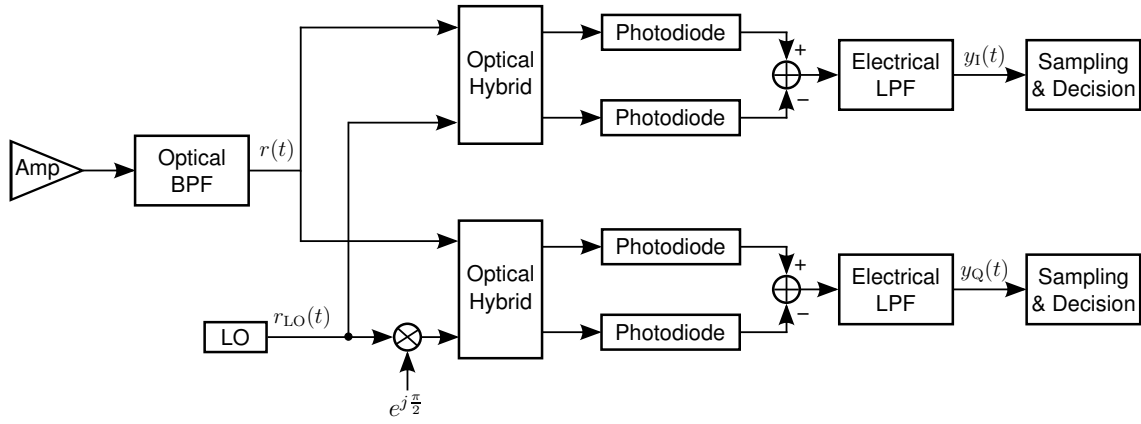
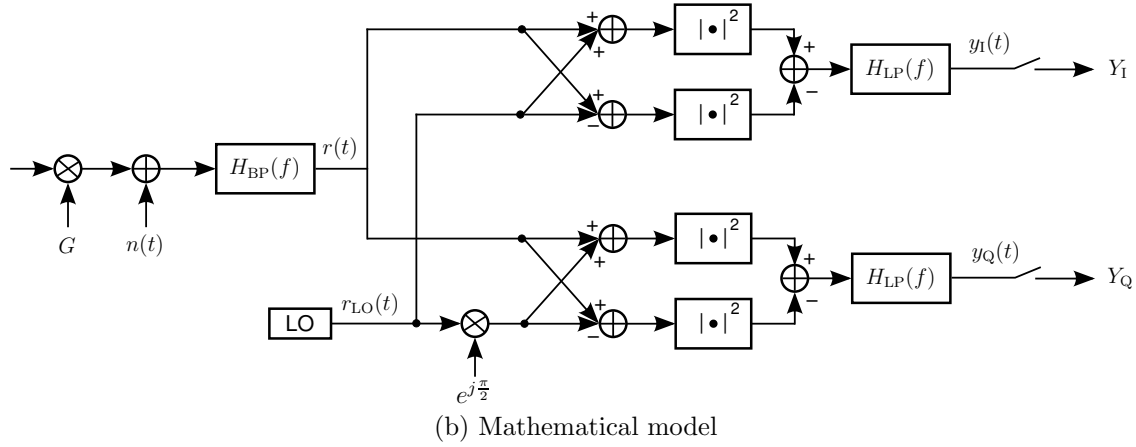


Figure 2.8: Effect of CD on the QPSK (left) and 16-QAM (right) constellation diagrams using E33 pulse-shaping filter. $\beta_2 = 22$ ps²/km.



(a) Block diagram



(b) Mathematical model

Figure 2.9: Coherent optical I/Q demodulator [3].

carrier frequency and the LO signal frequency.

The optical amplifier which is commonly used is the Erbium doped fiber amplifier (EDFA). The EDFA amplifier, with gain G , contributes in some optical noise, $n(t)$, which is modeled as an additive white Gaussian noise (AWGN) with single-sided power spectral density $N_0 = \frac{F}{2} h\nu G$, where h is Planck's constant, ν is the frequency of the light, and F is the noise figure. The signal-to-noise ratio (SNR) at the amplifier output is less than the amplifier input. Noise figure shows how much noise the amplifier adds to the input signal and is defined as $F = \frac{\text{SNR}_{\text{in}}}{\text{SNR}_{\text{out}}}$, in which SNR_{in} and SNR_{out} are the SNR at the amplifier input and output respectively [2, Chap. 6].

A Gaussian filter is used as the optical bandpass filter for filtering out the noise caused by EDFA. The baseband frequency response of such a filter for a passband system with 3-dB bandwidth B is [3]

$$H_{\text{BP}}(f) = e^{-\frac{2 \log_e 2}{B^2} f^2}. \quad (2.19)$$

The purpose of the electrical lowpass filter, H_{LP} , is to filter out the high frequency components after the photodiode operation. There is a trade off in choosing the bandwidth of the bandpass and lowpass filters. Larger bandwidths of the filters

lead to more noise in the system and consequently the performance of the system degrades. On the other hand filter bandwidths lower than the signal bandwidth result in distortion and ISI. In this thesis we use a lowpass filter which is matched to the pulse-shaping filter.

Considering the mathematical model of the homodyne coherent receiver shown in Figure 2.9b and considering no noise in the system we can write the following expressions:

$$r(t) = A(t) \cos(\omega_c t + \phi(t)) \quad (2.20)$$

$$r_{LO}(t) = A_{LO} \cos(\omega_c t). \quad (2.21)$$

where $r(t)$ is the received signal, $A(t)$ and $\phi(t)$ are the amplitude and phase of the received signal, ω_c is the carrier frequency, and A_{LO} is the amplitude of the local oscillator. Also, after lowpass filtering the photodiodes outputs we get the desired inphase and quadrature signals given by

$$y_I(t) = A_{LO}A(t) \cos \phi(t) \quad (2.22)$$

$$y_Q(t) = A_{LO}A(t) \sin \phi(t). \quad (2.23)$$

Then these filtered signals are sampled at maximum eye opening and decisions are made base on the samples.

2.4 LITERATURE STUDY ON CHROMATIC DISPERSION COMPENSATION

Chromatic dispersion can be compensated in either optical or electrical domain. The optical domain compensation is done via using dispersion compensating fibers (DCF) [2, pp. 436–437] or optical equalizing filters such as interferometric filters [2, pp. 438–440] or fiber Bragg gratings [2, pp. 441–448]. The shortcomings with the optical compensation are high loss, degraded performance, costly optical compensators and amplifiers, and sizeable equipments. Thus compensating fiber dispersion by using electronic digital signal processing (DSP) avoids the requirement for bulky, expensive and high loss optical dispersion compensation components, as well as providing adaptive filtering methods and advantages of high functionality, simpler deployment and reconfiguration, and reproducibility of the system [9] [10]. High bit rates in optical communications put limitation in the use of DSPs. However, today the continuing rapid development of integrated circuits and digital technology allows implementing DSPs that can operate in such high rates with acceptable power consumption.

As we saw in Section 2.2.2, dispersion can be approximately considered as a linear operation. So it can be compensated with a linear filter that mimics the inverse chromatic dispersion response. Actually electronic dispersion compensation (EDC) has been accomplished with different approaches: using linear FIR filters [8, 10] at

transmitter or receiver side or using nonlinear filters based on look-up tables (LUTs) at the transmitter [9]. Digital infinite impulse response (IIR) filtering as a means for EDC is also proposed in [11] which claims using a significantly smaller number of taps compared to FIR filters. Furthermore, real-time systems employing linear and nonlinear filters in a single-mode fiber have also been implemented in [12] and [13] respectively.

Performing EDC at the receiver has a limited performance in direct-detection systems as the optical phase information is lost due to square operation of photo detector [14]. However some systems have been proposed based on feed-forward equalizers (FFE) and decision-feedback equalizers (DFE) to compensate CD after direct-detection [15, 16]. Over the last few years, transmitter-side implementation of EDC has attracted a lot of attention since electronic predistortion (EPD) is a simpler technique and results in less complex receivers which is more desirable [14].

Large amount of required memory is a main drawback in LUT-based systems as the memory size is exponentially proportional to the amount of dispersion, while the size of the linear filter scales linearly with the dispersion of the link [14]. However exploiting the LUT approach to compensate nonlinear effects such as SPM is inevitable [4]. Therefore, a reasonable approach is to compensate CD by linear filtering and compensate nonlinear effects by LUT-based nonlinear filters [14, 17]. As in nonlinearity compensation only a limited number of adjacent bits needs to be taken into account, the size of LUT will not be so large in this case.

In the next chapter we consider EDC using a real-time FIR filter. The filter can be employed in either the transmitter side (precompensation) or the receiver side (postcompensation). In this method compensation is done by (pre or post) distorting the signal using a linear filter whose transfer function is the inverse of CD, therefore at the receiver we will have the desired signal. In Chapter 4 we discuss further results on EDC using a nonlinear filter, where compensation is accomplished by predistorting the signal via using a LUT in the transmitter side.

3 CHROMATIC DISPERSION COMPENSATION BY LINEAR FILTERING

As mentioned before, CD is a linear phenomenon and can be compensated by using a FIR or an IIR linear filter. The linear filter can be deployed in either the transmitter side or the receiver side; the former is named precompensation while the later is known as postcompensation. In both pre and post compensation methods the filter applies the inverse effect of chromatic dispersion and consequently we have the desired signal without dispersion at the receiver.

3.1 SYSTEM MODEL

By adding a linear compensating filter to the optical transmitter, previously shown in Figure 2.2, the structure of a precompensating transmitter system can be designed as shown in Figure 3.1. The I/Q modulator transfer function is given by Equation (2.4).

Compensation is done by pre-distorting the signal using the real-time linear FIR compensator which has the inverse chromatic dispersion transfer function. Therefore from Equations (2.17) and (2.18), the frequency and time response of the ICD filter can be respectively expressed as

$$H_{\text{icd}}(\omega) = e^{j\frac{\beta_2 d}{2}\omega^2} \tag{3.1}$$

$$h_{\text{icd}}(t) = \sqrt{\frac{j}{2\pi\beta_2 d}} e^{-j\frac{t^2}{2\beta_2 d}} \tag{3.2}$$

3.2 NUMBER OF FILTER TAPS

The design of a CD compensating filter in time domain and an upper bound on the number of taps required to compensate chromatic dispersion is obtained in [18].

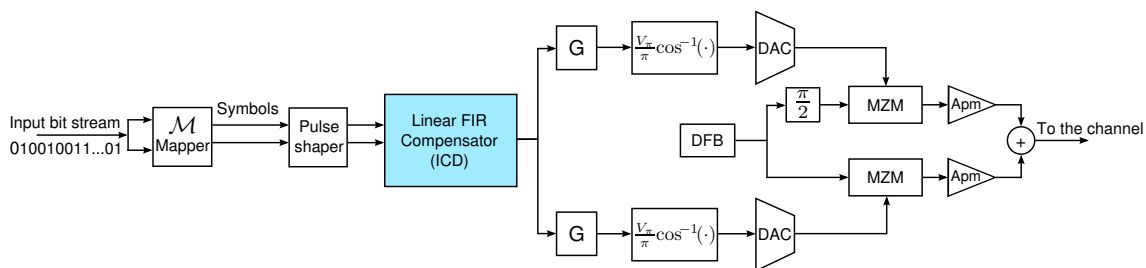


Figure 3.1: Schematic of the transmitter with linear FIR compensator.

With a similar method the minimum number of taps required to implement the compensating filter in time domain can be derived.

As the time response in Equation (3.2) and Figure 2.5 show, the frequency of the chirp increases continuously with time. Thus, to be able to sample it, first we have to window it. If we assume the double-sided bandwidth of the pulse shape is f_p , the window length should be chosen in a way that at least the maximum frequency of the pulse shape, $\frac{f_p}{2}$, is met in the chirp (see Figure 2.4), and the highest frequency component of the chirp, f_m , must be at most equal to half the sampling frequency, f_s , according to Nyquist sampling criterion. So we should have

$$\frac{f_p}{2} \leq f_m \leq \frac{f_s}{2} \quad (3.3)$$

Taking the derivative of the phase of Equation (3.2) with respect to time gives the angular frequency. So f_m can be expressed as [18]

$$f_m = \frac{1}{2\pi} \frac{d}{dt} \left(\frac{t^2}{2\beta_2 d} \right) \Big|_{t=t_m} = \frac{t_m}{2\pi\beta_2 d} \quad (3.4)$$

where t_m is the time at the far end of the truncated impulse response. From the above two equations we get

$$\pi\beta_2 d f_s f_p \leq \frac{t_m}{\Delta t} \leq \pi\beta_2 d f_s^2 \quad (3.5)$$

where $\Delta t = \frac{1}{f_s}$.

If we assume the one-sided number of taps is n_1 , i.e. $n_1 \Delta t \leq t_m \leq (n_1 + 1) \Delta t$, then the total number of taps will be $N = 2n_1 + 1$, and we have the following criterions directly derived from Inequality (3.5)

$$\lceil \pi\beta_2 d f_s f_p \rceil \leq n_1 \leq \lfloor \pi\beta_2 d f_s^2 \rfloor \quad (3.6)$$

$$2 \times \lceil \pi\beta_2 d f_s f_p \rceil + 1 \leq N \leq 2 \times \lfloor \pi\beta_2 d f_s^2 \rfloor + 1 \quad (3.7)$$

where $\lceil x \rceil$ is the nearest integer greater than or equal to x and $\lfloor x \rfloor$ is the integer part of x .

According to the latest inequality the bounds for the number of filter taps are functions of sampling frequency. By considering the minimum sampling frequency allowed, i.e. $f_s = f_p$, the minimum possible number of taps that can be used to implement the CD compensating filter can be expressed as follows

$$N = 2 \times \lfloor \pi\beta_2 d f_p^2 \rfloor + 1 \quad (3.8)$$

Thus the minimum possible number of taps is a function of pulse shape bandwidth, f_p . The bandwidths of some common pulse shapes are compared in Figure 2.4. The minimum possible number of taps given by above equation are also illustrated in Figure 3.2 using different pulse shapes and at different fiber lengths. The bandwidth of the RRC pulse is $\frac{1+\alpha}{T_s}$. The bandwidth of the Gaussian pulse (with 80% of its

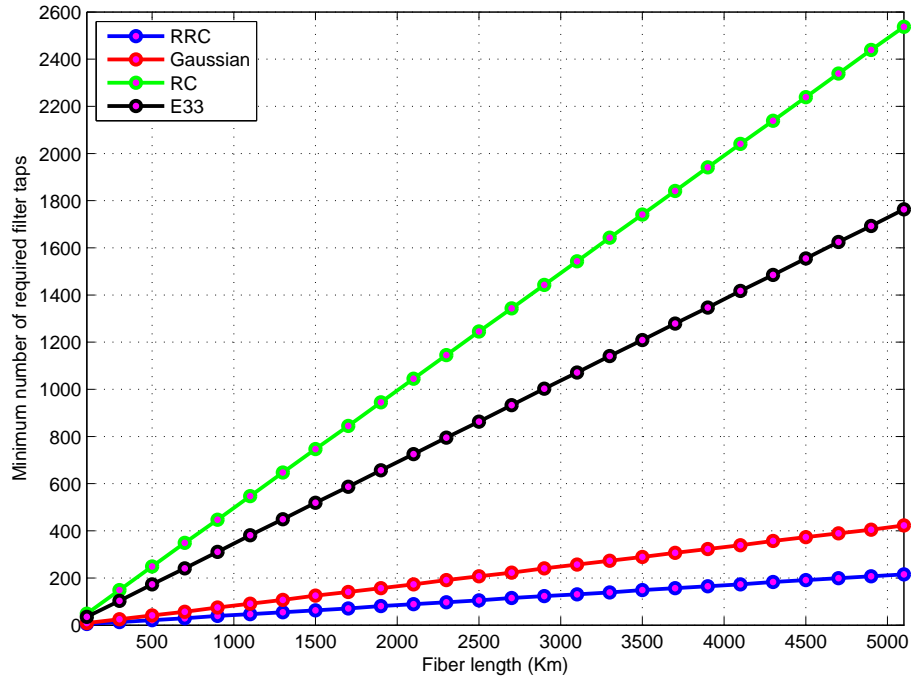


Figure 3.2: The minimum number of taps required at different fiber lengths for a FIR compensating filter in a 10 Gbaud/s optical transmitter. $\beta_2 = 22 \text{ ps}^2/\text{km}$. The pulse-shaping filters used are: (RRC pulse with $\alpha = 0.75$ and $f_p = (1 + \alpha)/T_s$, Gaussian pulse with 80% of its energy contained in the symbol time and $f_p = 2.44/T_s$, RC in time domain with $\alpha = 0.75$ and $f_p = 6/T_s$, and E33 pulse with $f_p = 5/T_s$).

energy contained in one symbol time) is chosen to be $\frac{2.44}{T_s}$ so that it contains 99% of its energy. The bandwidths of RC (in time domain) and E33 pulse are also considered $\frac{6}{T_s}$ and $\frac{5}{T_s}$ respectively. This figure shows that using a narrow-band pulse such as RRC, can decrease the minimum possible number of taps and thus the complexity of the filter, for example for over 5000 km of fiber with $\beta_2 = 22 \text{ ps}^2/\text{km}$ in a 10 Gbaud/s system only around 200 taps are needed if the RRC pulse is used.

Truncating the impulse response to less than the limit given by Equation (3.7) destroys the signal bandwidth and leads to distortion and ISI. On the other hand going further the upper limit causes aliasing as the Nyquist sampling theorem is not met anymore.

3.3 TIME-DOMAIN AND FREQUENCY-DOMAIN IMPLEMENTATIONS

As mentioned before, the linear compensating filter can be implemented in either time or frequency domain. The time-domain implementation and the required number of taps are discussed in the previous section. For the frequency-domain implementation the Equation (3.1) is directly employed, sampled and multiplied in the

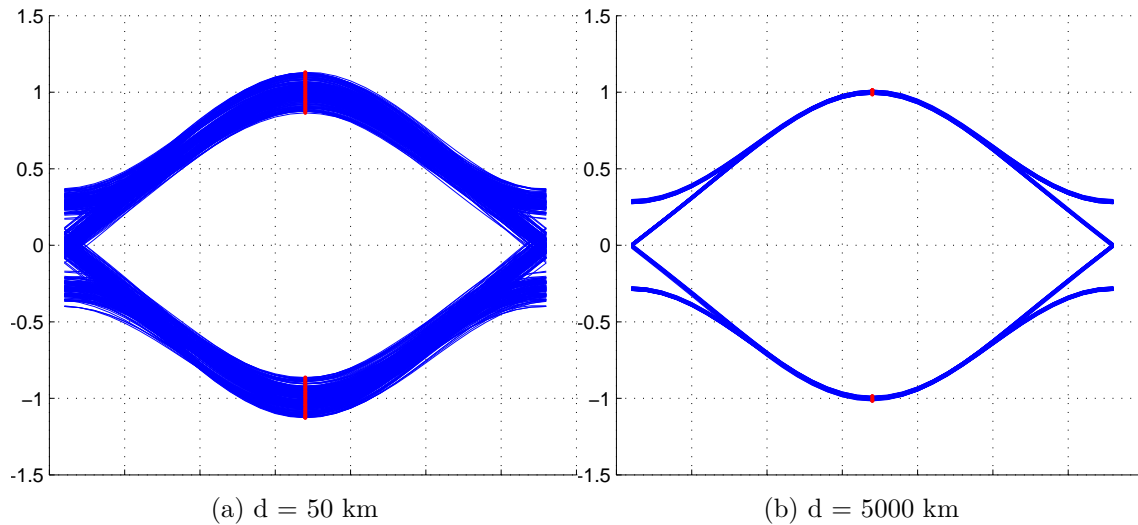


Figure 3.3: The effect of windowing the compensating filter on the eye diagram of a QPSK system at a lower fiber length (left) compared to the negligible windowing effect at a higher fiber length (right). Red points are the symbol times.

transfer function of the filter input. In contrast to the time-domain implementation of the compensating filter, there is no upper limit for the number of filter taps in frequency domain since the input signal to the compensating filter is band-limited. To have a fair comparison between time and frequency domain implementations of the compensating filter (i.e. to have the same number of filter taps for both), the linear compensating filter is implemented for realtime processing by using the overlap-save technique. In this technique the large input stream to the filter is broken into blocks of shorter lengths. The outputs of successive blocks are computed and concatenated in a proper way to generate the total output. This method also reduces the runtime significantly.

Windowing effect in time-domain implementation of the filter is inevitable when the number of taps is not large enough and this causes a small deviation from the actual transfer function of ICD filter given by (3.1). Figure 3.3 shows the windowing effect of implementing the compensating filter in time domain on the eye diagram when the minimum number of taps given by Equation (3.7) is used in a QPSK system. Figure 3.4 also shows the eye diagrams at the same fiber lengths, but here the compensating filter is implemented in the frequency domain. It can be seen in Figure 3.3a that at lower fiber lengths the eye is more closed compared to the eye at higher lengths when the time-domain filter is used (Figure 3.3b), or compared to the eye diagram when the frequency-domain filter at the same filter length is used (Figure 3.4a). Since at higher lengths of fiber the number of taps is large and the truncation length is long enough, the windowing effect is negligible.

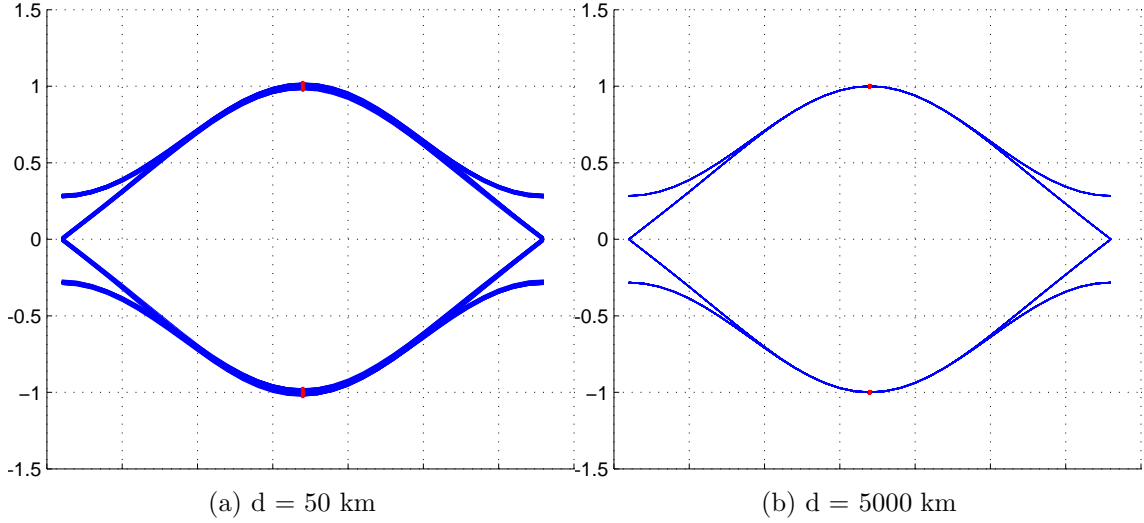


Figure 3.4: Eye diagram of a QPSK system at two different fiber lengths when the compensating filter is implemented in frequency domain. Red points are the symbol times.

3.4 EFFECT OF FILTERING ON THE AMPLITUDE

The cosine function of I/Q modulator, as stated in equation (2.4), is compensated by using an inverse cosine block before it, as shown in Figure 3.1. This can be implemented using a small LUT. As the input to the inverse cosine function can only have the values between -1 and 1, the amplitude of the signal after the compensating filter must be normalized to fall within this range which is done by block **G** in Figure 3.1. Here for normalizing the amplitude, we need to calculate the maximum amplitude generated after the compensating filter. The output of the filter can be written as

$$r = \sum_{n=0}^{L-1} s_n (p(t - nT_s) * h_{\text{icd}}(t)) = \sum_{n=0}^{L-1} s_n x(t - nT_s) \quad (3.9)$$

where s_n is n 'th transmitted symbol, L is the total number of symbols to be transmitted, T_s is the symbol duration, $p(t)$ is the pulse shape, $x(t) = p(t) * h_{\text{icd}}(t)$, and $h_{\text{icd}}(t)$ is the inverse time response of CD given by (3.2). By assuming $s_n = s_{n,r} + js_{n,i}$ and $x(t) = x_r(t) + jx_i(t)$ the maximum amplitude of the inphase signal can be expressed as

$$A_{\text{max,inphase}} = \max(\mathbf{Re}\{r\}) = \max\left(\sum_{n=0}^{L-1} s_{n,r}x_r(t - nT_s) - s_{n,i}x_i(t - nT_s)\right) \quad (3.10)$$

The maximum amplitude of the quadrature signal can be derived in a similar way. By symmetry we can say the maximum amplitude of the inphase signal is the same

as the quadrature signal and is given by

$$A_{\max, \text{inphase}} = A_{\max, \text{quadrature}} = \max_{1 \leq l_0 \leq l_s} \left\{ \sum_{n=1}^K B \left[|x_r(l_0 + (n-1)l_s)| + |x_i(l_0 + (n-1)l_s)| \right] \right\} \quad (3.11)$$

where $B = \max(s_{n,r}) = \max(s_{n,i})$ and depends on the modulation scheme. For QPSK and 16-QAM modulations B is typically 1 and 3 respectively. $l_s = \lceil \frac{T_s}{\Delta t} \rceil$ which is the number of samples per symbol and

$$K = \left\lceil \frac{N\Delta t + T_p}{T_s} \right\rceil \quad (3.12)$$

in which $\lceil x \rceil$ is the nearest integer greater than or equal to x , T_p is the time duration of pulse $p(t)$ and N is defined according to equation (3.7). K can also be interpreted as the number of adjacent symbols that contribute to the ISI.

A specific input bit pattern results in the maximum amplitude derived by (3.11). The probability that such a pattern occurs can be very low as this probability decreases exponentially by increasing dispersion depth (K). This probability can be expressed as $P_{A_{\max}} = \frac{2}{M^K}$ where M is the number of constellation points (e.g., $M = 4$ in a QPSK and $M = 16$ in a 16-QAM system) and K , as calculated above, depends on time duration of the compensating filter and the pulse $p(t)$.

The effect of compensating filter on the maximum amplitude of the signal is illustrated in Figure 3.5. Figures 3.5a and 3.5b show the ratio $\frac{A_{\max}}{A_p}$ for 16-QAM, QPSK, BPSK, and OOK modulation schemes at different fiber lengths, where A_p and A_{\max} are the maximum amplitudes of the signal before and after filtering respectively. The simulations are done with different pulses: The RRC pulse with $\alpha = 0.75$, the Gaussian pulse with 80% of its energy included in each symbol duration, RC (in time domain) with $\alpha = 0.75$, and the E33 pulse. Figures 3.5c and 3.5d also show the maximum amplitude generated after the compensating filter, if unit energy pulses are used.

3.5 PERFORMANCE OF LINEAR PRECOMPENSATING METHOD

The simulated performance of the QPSK and 16-QAM systems at different fiber lengths using the system model of Figure 3.1 are shown in Figures 3.6 and 3.7 respectively. As the curves show, the performances of each system is the same as what theory indicates (regardless of filter implementation in time or frequency domain), which means that the fiber dispersion is completely compensated. The theory curves indicate the performance of the systems using Gray coding and operating in white noise when there is no dispersion or in other words when the the fiber length is set to zero.

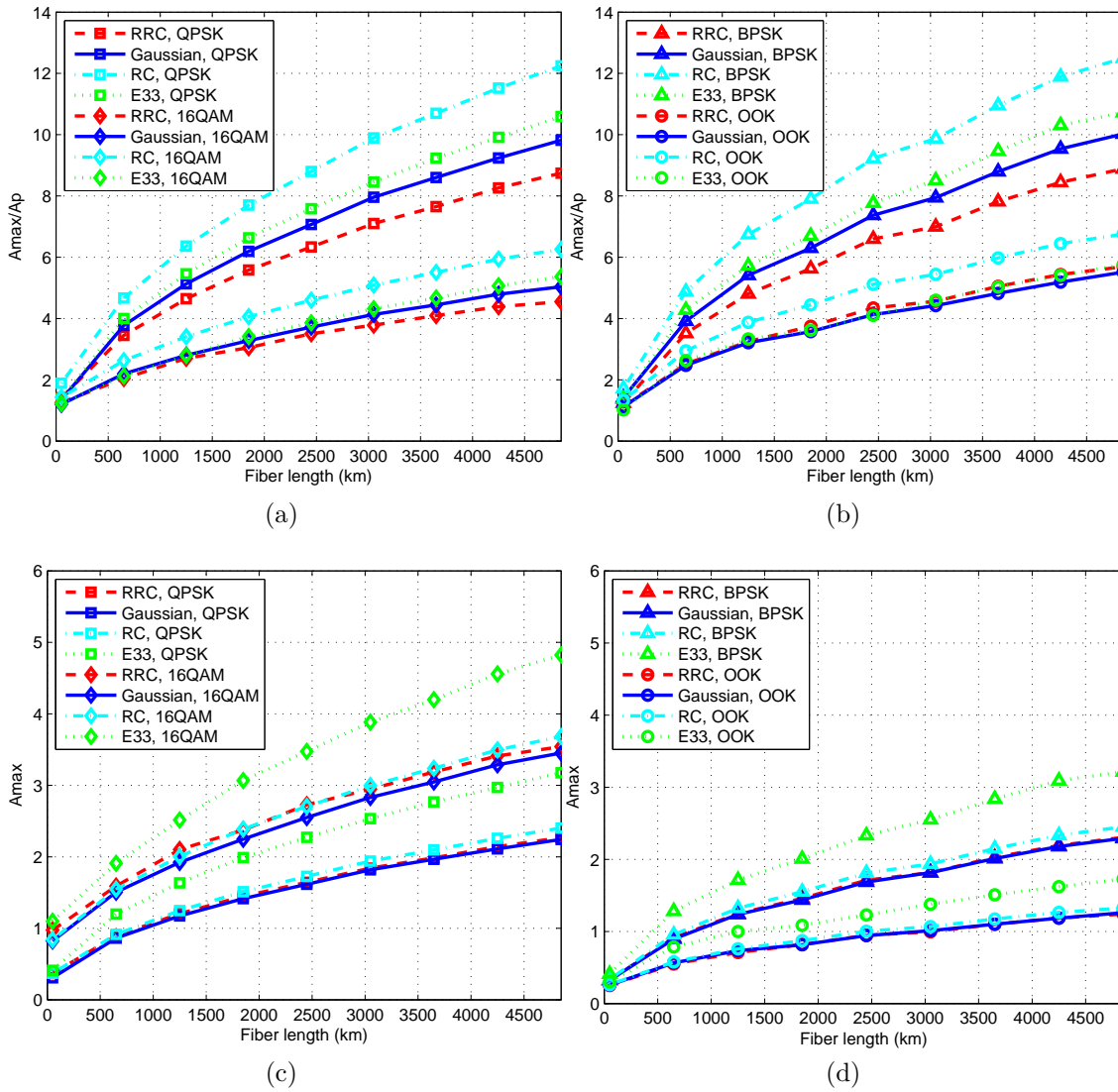


Figure 3.5: The effect of compensating filter on amplitude of the signal in different modulation schemes using RRC ($\alpha = 0.75$), Gaussian (80% of its energy included in each symbol duration), RC in time domain ($\alpha = 0.75$), and E33 pulses.

3.5.1 THE EFFECT OF D/A RESOLUTION ON THE PERFORMANCE

According to the system model in Figure 3.1, a digital-to-analog converter (DAC) is used after the inverse cosine block to generate the analog drive signals of the MZMs from digital samples of the predistorted signal. The analog value of the signal after the DAC will always differ from the quantized digital value before and the difference is called quantization error. Higher resolutions (i.e. the number of bits, b , used for each sample) in DACs leads to less quantization error. Figures 3.8 and 3.9 show the effect of DAC resolution on the performance of the QPSK and 16-QAM linear precompensation systems at 5000km fiber length respectively. It can be seen that

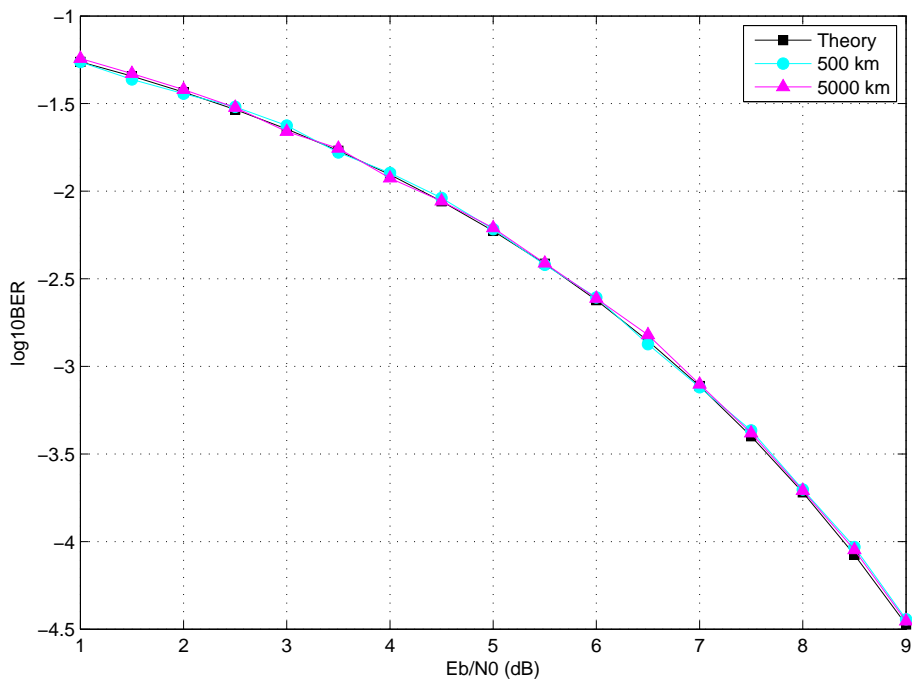


Figure 3.6: BER vs. SNR in a QPSK linear precompensation system at 0km, 500km, and 5000km fiber lengths.

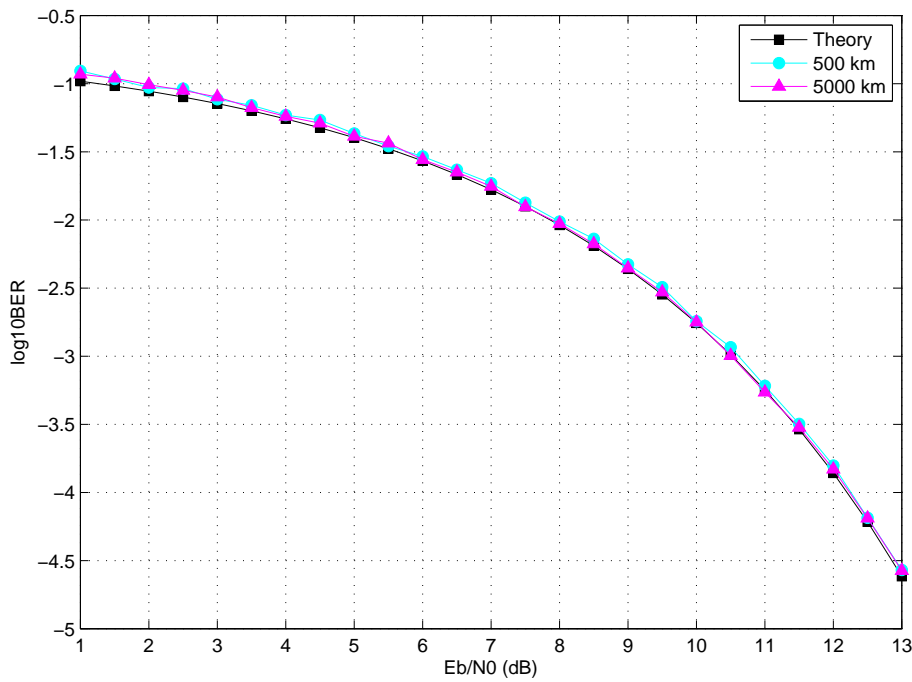


Figure 3.7: BER vs. SNR in a 16-QAM linear precompensation system at 0km, 500km, and 5000km fiber lengths

in the QPSK system using a 4-bit or higher resolution DAC does not degrade the performance. For the 16-QAM system 1 more bit is needed as the input range to

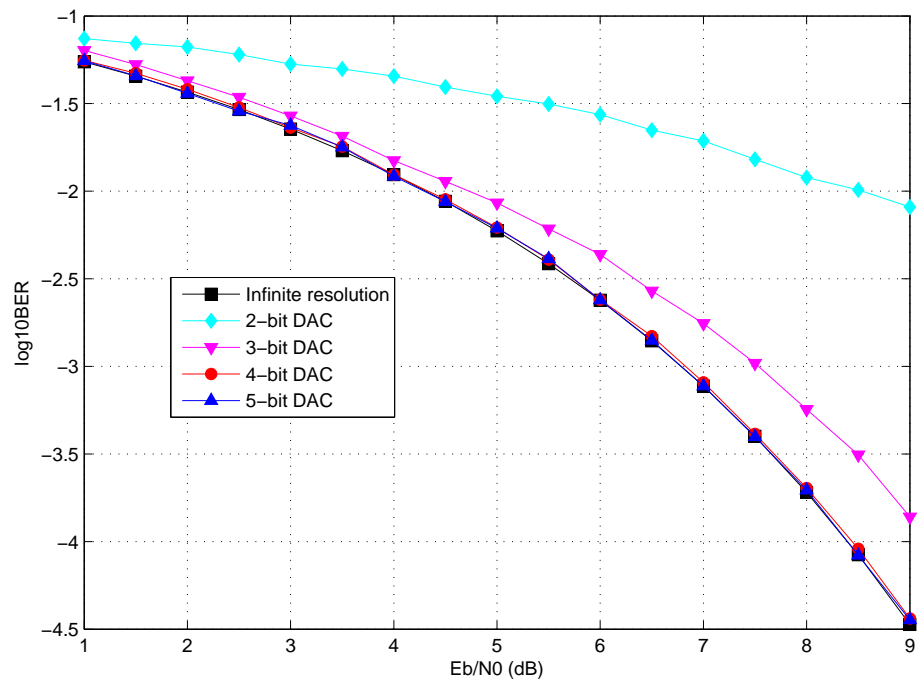


Figure 3.8: BER comparison of a QPSK system using 2, 3, 4, and 5-bit DAC at 5000km fiber lengths.

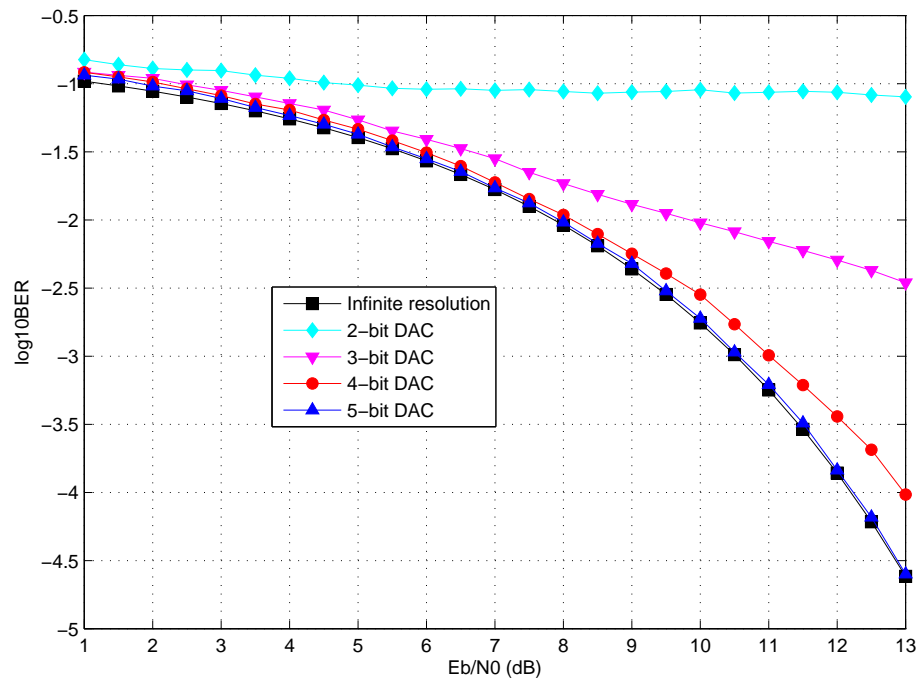


Figure 3.9: BER comparison of a 16-QAM system using 2, 3, 4, and 5-bit DAC at 5000km fiber length

the DAC is larger compared to the QPSK system. Here, with a 5-bit DAC we don't lose the performance.

4 CHROMATIC DISPERSION COMPENSATION BY NONLINEAR FILTERING

Look-up tables can be used as general nonlinear filters if the input signal can only assume a finite number of values. As mentioned before, chromatic dispersion has also been compensated using a look-up table [9]. The drawback with this approach is the large amount of memory required for the LUT since in CD compensation the number of bits that need to be taken into account can be large [14]. But on the other hand the advantage of using LUTs is that they can be used to compensate nonlinear effects such as higher order dispersions and SPM.

In [19] it is shown that the LUT generated for compensating CD in dispersion-limited links can be significantly compressed by applying the Hadamard transform. In this chapter we discuss further results on what has been done in [1] and [19].

4.1 THE TRANSMITTER SYSTEM MODEL

The system model of the transmitter with compensation employing LUT is shown in Figure 4.1. As described in [1], if we assume l_s samples per symbol, then for each κ input symbols the LUT gives $2 \cdot l_s$ output samples corresponding to the predistorted middle symbol of the input sequence (the factor 2 is because of quadrature and inphase channels). Therefore by considering all input symbol patterns, we will have a LUT of size $2 \cdot M^\kappa \times l_s$ where M is the number of different symbols or in other words the number of constellation points.

The system design for generating the LUT is shown in Figure 4.2. The inverse channel filter is the same as the compensating filter used in Chapter 3 and mimics the inverse behavior of the actual optical channel. The inverse cosine block is for compensating the cosine function of the Cartesian Mach-Zehnder modulator. As mentioned in Section 3.4, since the input to the inverse cosine can only be between -1 and 1, we should make sure that the amplitude of the signal after the inverse channel filter is always within this range.

4.2 THE CONSTRAINTS AND THE SOLUTIONS

By increasing the fiber length, the amount of dispersion increases. As a result, if we assume the baud rate is constant, more adjacent symbols interfere with each other according to Equation (3.12). Hence, to generate the LUT a longer input symbol sequence should be considered. As the size of LUT is exponentially dependent on the number of input symbols, κ , for high amounts of dispersion generating LUT

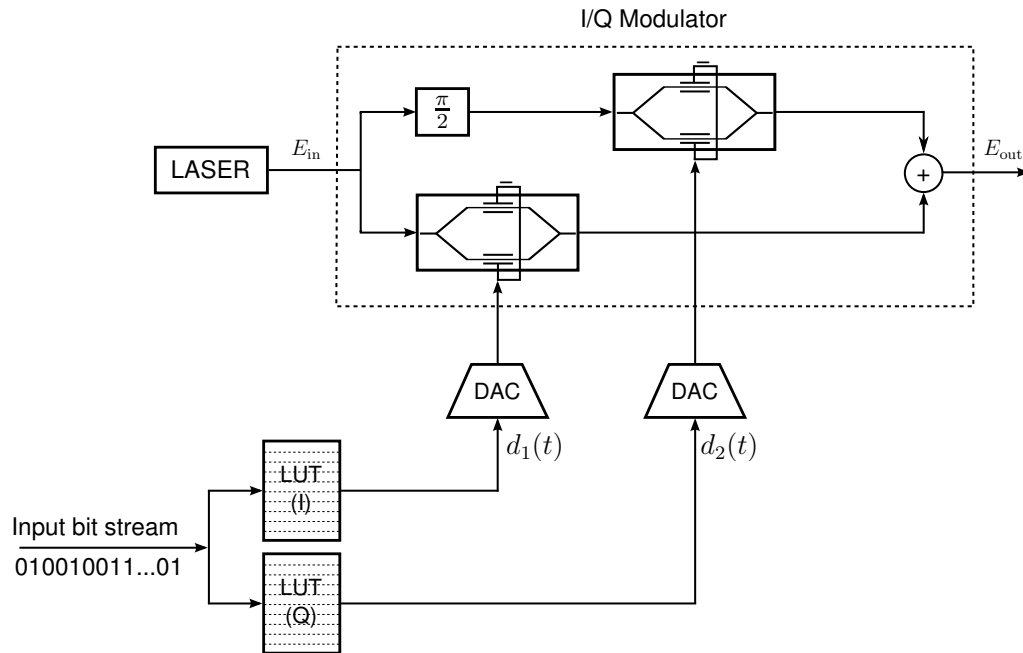


Figure 4.1: Schematic of optical transmitter with LUT-based compensator [1].

may not be feasible due to large memory requirements.

A method for compressing the LUT with the Hadamard transform has been proposed in [1] and [19] which greatly reduces the size of memory and scales it linearly with the number of input symbols. So instead of using LUT in the system model of Figure 4.1, the compressed look-up table (CLUT) can be replaced. More details on how the CLUT is generated and how the reconstruction of LUT from CLUT is done can be found on [1]. Although the main solution to the memory constraint is given by the Hadamard transform technique, there are still some constraints in implementing such a system. Here I introduce these constraints and I discuss about some implementation details to avoid some of these constraints.

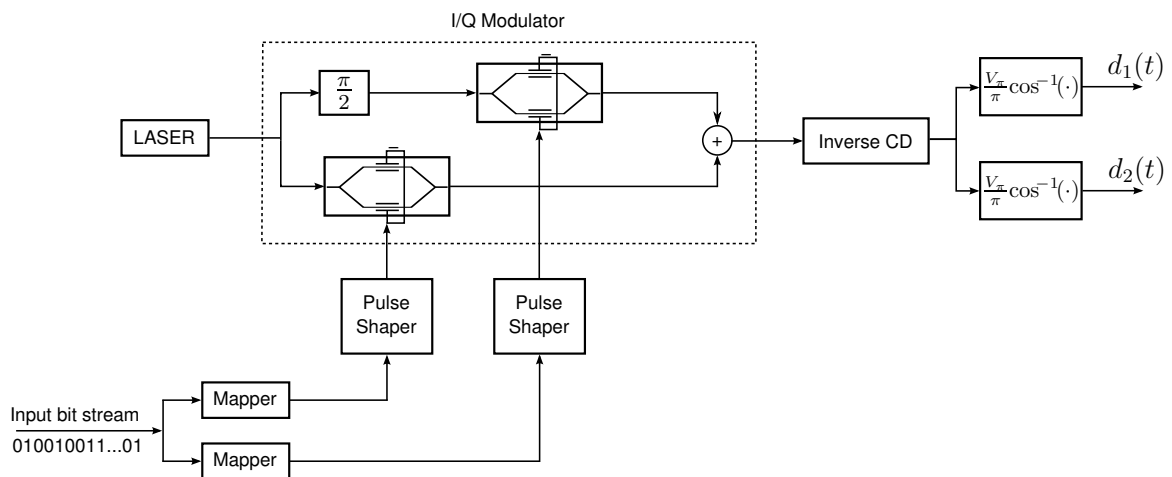


Figure 4.2: Schematic of the system for generating LUT [1].

As mentioned in [1], to generate the LUT with M^κ rows, a very long symbol sequence, which guarantees that all the κ symbol patterns are contained in it, is generated. Using a pseudo random binary sequence (PRBS), in best case a bit sequence of length $\log M \times M^\kappa$ is needed to include all the symbol patterns. If κ gets large this can be a very large sequence, especially after upsampling, and it can introduce memory constraints for saving such a long vector. Another constraint can be the processing time for filtering such large number of samples. Here the processing time can be reduced by real-time processing implementation of the filter as partially described in Section 3.3.

As depicted in Figure 4.3a, after generating the long waveform corresponding to the large input symbol sequence, the CLUT can be generated in two ways. One way is generating LUT first, and then applying the Hadamard transform to it to get a table of the same size but with lots of zero-value rows. Next, the nonzero rows of the transformed LUT form the compressed table, CLUT. Here, again we encounter memory constraint in generating CLUT, since the large-size LUT have to be generated first.

To avoid the large memory requirement introduced by the LUT, we should consider generating CLUT directly from the long predistorted waveform. As mentioned before, LUT is generated in the following way that each time we look for a part of the long predistorted waveform that corresponds to the middle symbol in the κ input symbol sequence and we save that part in a row of LUT defined by the κ input symbol sequence. After filling all the LUT rows in this way, we apply the Hadamard transform to it to compress it. After taking the Hadamard transform of the LUT, most of the rows have zero values and they can be skipped.

Now, to avoid generating LUT we can do the following. We know what the significant Hadamard components are (the nonzero rows) [1], and we know that each element of the Hadamard matrix is given by

$$(\mathbb{H})_{i,j} = (-1)^{\sum_k i_k j_k} \quad (4.1)$$

where $(\mathbb{H})_{i,j}$ is the element (i, j) of the Hadamard matrix \mathbb{H} , and i_k and j_k are k 'th bits in the base-2 representation of i and j respectively. Each time that we find the predistorted waveform corresponding to the middle symbol in the κ input symbol sequence, we can perform some part of required calculations for generating CLUT instead of saving it in a row of the LUT. So for each extracted waveform from the long predistorted waveform, some part of each CLUT element is calculated and added to the previous value of that element. This is shown in Figure 4.3a where CLUT is generated from the long waveform in one step.

So far we have removed the need for generating the LUT before generating CLUT. But as discussed before, still the long input symbol sequence introduces a memory size constraint. Figure 4.3b shows another way of generating LUT. Instead of generating a long bit sequence that contains all κ symbol sequence patterns, we can generate M^κ different sequences of length κ symbols and construct each LUT row by applying each of these sequences in a loop.

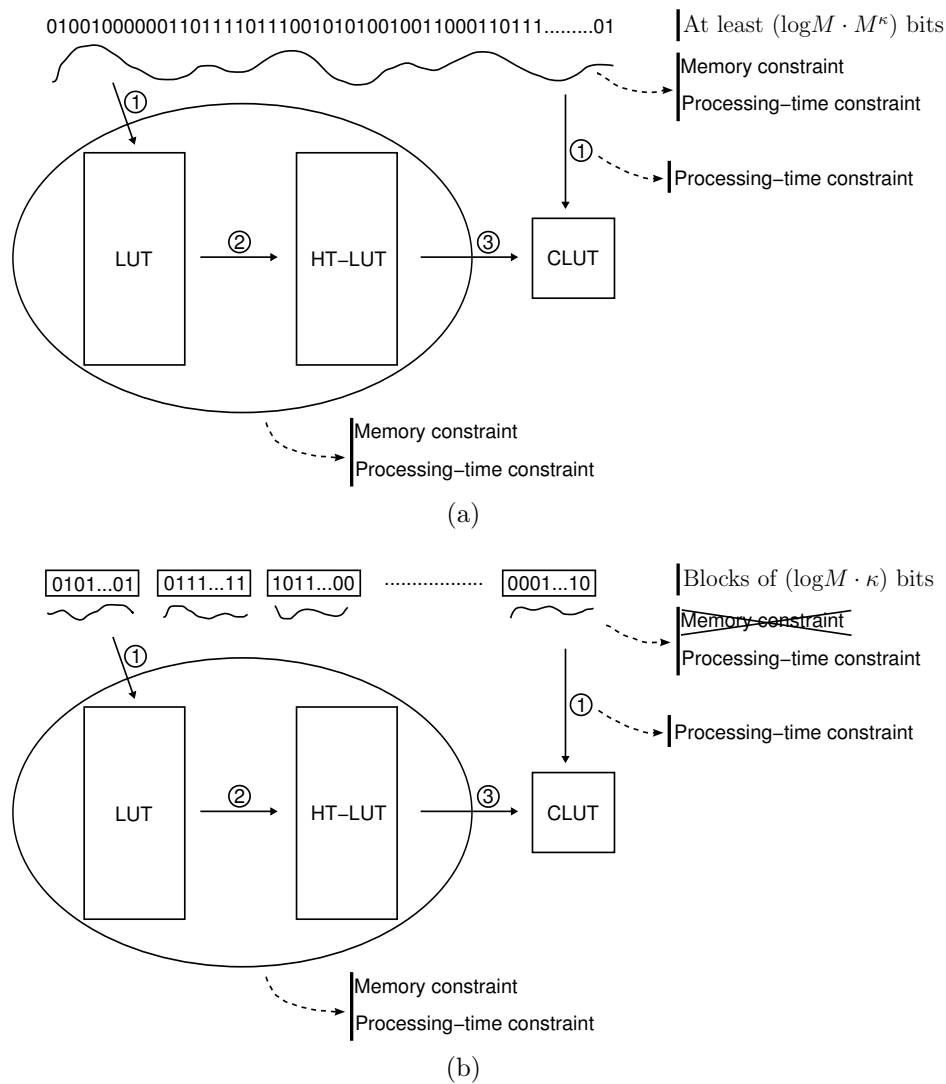


Figure 4.3: Generating CLUT from a long input bit stream (a) or from smaller size blocks of bits (b).

In a case that the number of symbols, κ , in the input symbol sequence of LUT is less than the actual number of symbols that should be considered, K in Equation (3.12), some random symbols can be concatenated to the input symbol sequence in order not to lose the advantage of averaging that the Hadamard transform performs in generating the CLUT.

In this way of generating the LUT, again we can apply the previously discussed implementation technique to generate CLUT directly without first generating LUT. Therefore, finally by breaking the long input sequence to smaller sequences and by realtime calculation of CLUT elements we do not face any memory limitation in the implementation anymore. Although still the processing time can be very large if κ gets large, we should notice that this time is only spent once at the start-up.

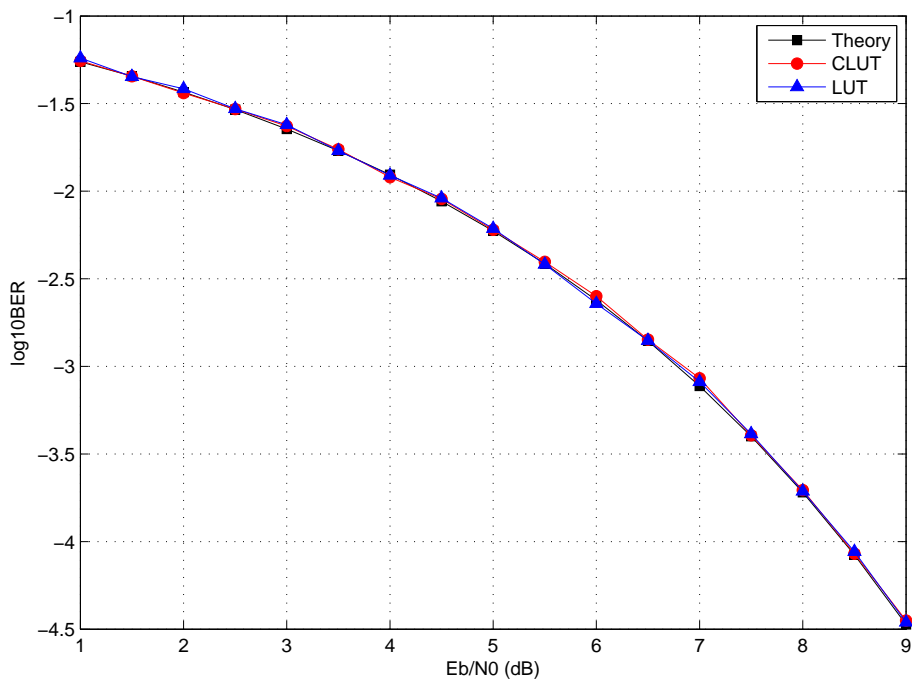


Figure 4.4: Comparing BER of QPSK systems with compression (CLUT) and without compression (LUT) when the block size (=14 bits) is adequate regarding the fiber length ($d = 200$ km).

4.3 PERFORMANCE OF NONLINEAR PRECOMPENSATING METHOD

The LUT-based precompensation system with QPSK modulation format working at 10 Gbaud is simulated. The input symbol sequence to the LUT is set to 7 symbols, i.e. 14 bits, and CLUT is directly generated as described in the previous section. Thus by taking 32 samples per symbol, i.e. $l_s = 32$, the dimensions of LUT and CLUT are $2 \cdot 2^{14} \times 32$ and $2 \cdot (14 + 1) \times 32$ respectively. The performance of the system is tested in two different scenarios. First a lower value is chosen for the fiber length ($d = 100$ km) so that the symbol block size is adequate and contains all the adjacent interfering symbols. In this case the chromatic dispersion is completely compensated if either LUT or CLUT is used. This result is shown in Figure 4.4. Then by increasing the fiber length to ($d = 500$ km), the system is simulated for a case that the symbol block size is less than the actual number of adjacent symbols that interfere with each other. As shown in Figure 4.5, in this case there is some degradation in the performance of the system as the CD is not compensated completely. The more affected symbols by dispersion ignored, the more degradation in performance we will have. As discussed in [19] and [1], the performance of the system using CLUT is better than the system with LUT because of the averaging property of the Hadamard transform.

As previously mentioned, by removing the memory constraint, larger lengths of

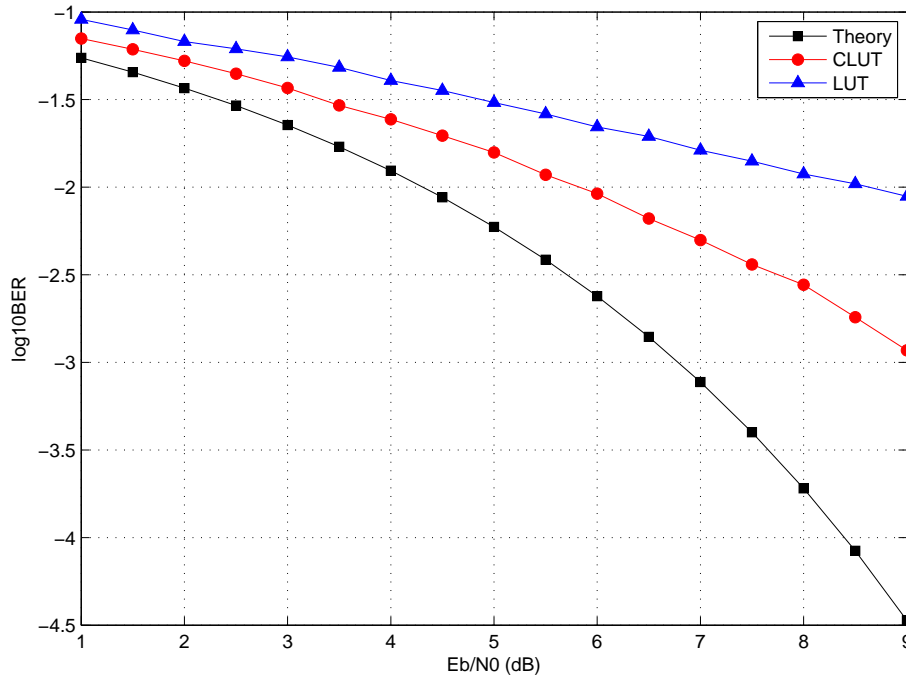


Figure 4.5: Comparing BER of QPSK systems with compression (CLUT) and without compression (LUT) when the block size (=14 bits) is inadequate regarding the fiber length ($d = 500$ km).

input sequence to the LUT can be applied. In Figure 4.6 we see that by increasing the block size to 22 bits, the CD that could not be compensated in the previously with a lower block size, is now completely compensated.

4.4 COMPARING WITH LINEAR COMPENSATION, PROS AND CONS

If we assume that the number of adjacent symbols affected by dispersion is K according to Equation (3.12), the total memory requirement for the nonlinear filtering method without compression is given by $2 \cdot M^K l_s b$, where M is the number of constellation points, l_s is the number of samples per symbol, b is the D/A resolution, and the factor 2 implies real and imaginary parts. The computational complexity can be high at the start-up for generating the LUT if the table size is large, but the runtime complexity is very low as it only includes reading from a memory. Generating a LUT for high amount of dispersion may not be feasible because of limitations in storage capacity and also huge processing time.

The nonlinear filtering with direct compression requires much lower memory. The total memory requirement is given by $2 \cdot \log M \cdot K l_s b$. The startup and runtime computational complexities are higher compared to the method without compression as the Hadamard and inverse Hadamard transforms are involved in them respectively.

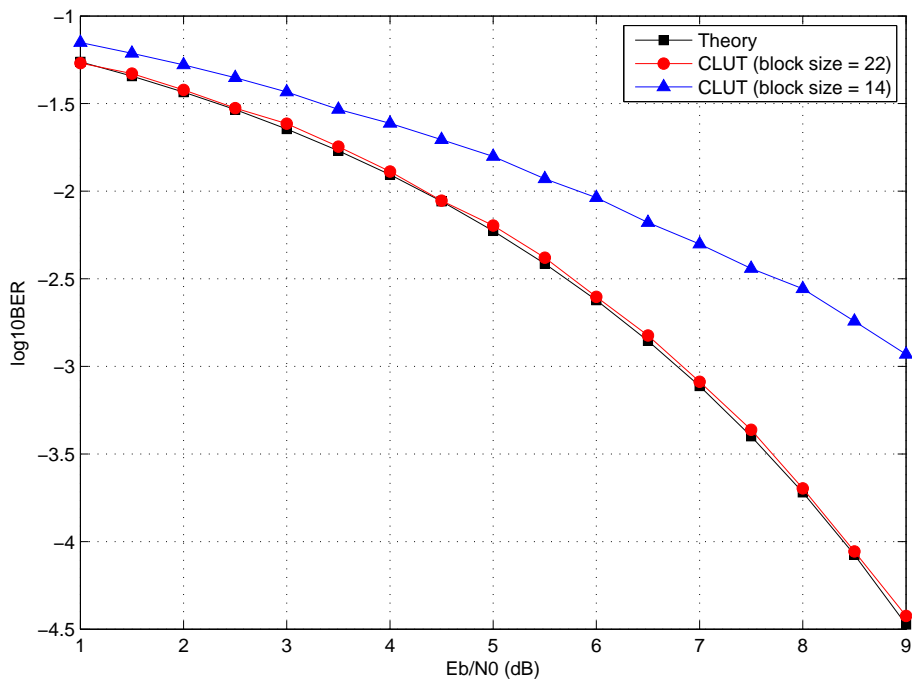


Figure 4.6: BER of QPSK systems for a larger block size (=22 bits) compared to the previously used smaller block size (=14 bits) in 500 km fiber length.

Although more dispersion can be compensated with this approach, generating CLUT can also be infeasible at high amounts of dispersion due to the huge computational complexity.

Finally, the memory requirements for the linear filtering method is $2 \cdot Nb$ or equivalently $2 \cdot Kl_s b$ where N is the number of filter taps and is defined in Equation (3.7). The runtime complexity is higher than the nonlinear filtering method as filtering the signal is continuously done in the transmitter. The advantage with this approach is that even high amounts of dispersion can be completely compensated as the number of filter taps is very high in most of the cases.

5 CONCLUSIONS

Chromatic dispersion is a linear phenomenon and can be fully compensated by using linear FIR filters to predistort the signal. Reasonable number of taps is needed even for high amounts of dispersion if a narrow-band signal is used. In the lookup table-base compensation method, chromatic dispersion can now be compensated for larger distances as the memory constraint is removed. Although look-up tables are usually used to compensate the nonlinear effects of the channel in a fiber optic system, chromatic dispersion compensation by using a compressed lookup table can also be of interest if the processing time for generating CLUT is not too much because this method has a low runtime computational complexity compared to linear filtering method. For example for a system working at 10 Gbaud and at 500 km fiber length the CLUT can be generated in reasonable amount of time so it should be preferred to the linear filtering method as it offers less runtime complexity. We also noticed that CLUT improves the performance of the system compared to LUT only if inadequate block size is chosen. Finally we saw that a 4-bit DAC in the QPSK and a 5-bit DAC in the 16-QAM system do not degrade the performance.

Bibliography

- [1] F. A. Khan, *Electronic dispersion compensation by signal predistortion using a compressed lookup table*. Master thesis, Department of Signals and Systems, Chalmers University of Technology, Goteborg, Sweden, 2009.
- [2] G. P. Agrawal, *Fiber-Optic Communication Systems*, 2nd ed. John Wiley and Sons Inc., New York, USA, 1997.
- [3] H. Zhao, *On Interference Suppression Techniques for Communication Systems*. PhD thesis, Department of Signals and Systems, Chalmers University of Technology, Goteborg, Sweden, 2008.
- [4] P. Watts, R. Waagemans, M. Glick, P. Bayvel, and R. Killey, “An FPGA-based optical transmitter design using real-time DSP for advanced signal formats and electronic predistortion,” *Journal of Lightwave Technology*, vol. 25, no. 10, pp. 3089–3099, Oct. 2007.
- [5] D. McGhan, M. O’Sullivan, M. Sotoodeh, A. Savchenko, C. Bontu, M. Belanger, and K. Roberts, “Electronic dispersion compensation,” in *Optical Fiber Communication Conference*, 2006.
- [6] J. B. Anderson, *Digital Transmission Engineering*, 2nd ed. John Wiley and Sons Inc., USA, 2004.
- [7] E. Ip and J. Kahn, “Power spectra of return-to-zero optical signals,” *Journal of Lightwave Technology*, vol. 24, no. 3, pp. 1610–1618, March 2006.
- [8] M. Said, J. Sitch, and M. Elmasry, “An electrically pre-equalized 10-Gb/s duobinary transmission system,” *Journal of Lightwave Technology*, vol. 23, no. 1, pp. 388–400, Jan. 2005.
- [9] R. Killey, P. Watts, V. Mikhailov, M. Glick, and P. Bayvel, “Electronic dispersion compensation by signal predistortion using digital processing and a dual-drive mach-zehnder modulator,” *IEEE Photonics Technology Letters*, vol. 17, no. 3, pp. 714–716, March 2005.
- [10] J. McNicol, M. O’Sullivan, K. Roberts, A. Comeau, D. McGhan, and L. Strawczynski, “Electrical domain compensation of optical dispersion,” in *Optical Fiber Communication Conference*, vol. 4, March 2005.
- [11] G. Goldfarb and G. Li, “Chromatic dispersion compensation using digital IIR filtering with coherent detection,” *IEEE Photonics Technology Letters*, vol. 19, no. 13, pp. 969–971, July 2007.
- [12] P. Watts, R. Waagemans, Y. Benlachtar, V. Mikhailov, P. Bayvel, and R. I. Killey, “10.7 Gb/s transmission over 1200 km of standard single-mode fiber by

- electronic predistortion using FPGA-based real-time digital signal processing,” *Opt. Express*, vol. 16, no. 16, pp. 12 171–12 180, Aug. 2008.
- [13] R. Waegemans, S. Herbst, L. Holbein, P. Watts, P. Bayvel, C. Fürst, and R. I. Killey, “10.7 Gb/s electronic predistortion transmitter using commercial FPGAs and D/A converters implementing real-time DSP for chromatic dispersion and SPM compensation,” *Opt. Express*, vol. 17, pp. 8630–8640, May 2009.
- [14] R. Killey, P. Watts, M. Glick, and P. Bayvel, “Electronic dispersion compensation by signal predistortion,” in *Optical Fiber Communication Conference*, March 2006.
- [15] P. Watts, V. Mikhailov, S. Savory, P. Bayvel, M. Glick, M. Lobel, B. Christensen, P. Kirkpatrick, S. Shang, and R. Killey, “Performance of single-mode fiber links using electronic feed-forward and decision feedback equalizers,” *IEEE Photonics Technology Letters*, vol. 17, no. 10, pp. 2206 – 2208, Oct. 2005.
- [16] J. Wang and J. Kahn, “Performance of electrical equalizers in optically amplified OOK and DPSK systems,” *IEEE Photonics Technology Letters*, vol. 16, no. 5, pp. 1397 –1399, May 2004.
- [17] D. McGhan, C. Laperle, A. Savchenko, C. Li, G. Mak, and M. O’Sullivan, “5120-km RZ-DPSK transmission over G.652 fiber at 10 Gb/s without optical dispersion compensation,” *IEEE Photonics Technology Letters*, vol. 18, no. 2, pp. 400 –402, 2006.
- [18] S. J. Savory, “Digital filters for coherent optical receivers,” *Opt. Express*, vol. 16, pp. 804–817, Jan. 2008.
- [19] F. A. Khan, E. Agrell, and M. Karlsson, “Electronic dispersion compensation by Hadamard transformation,” in *Optical Fiber Communication (OFC), collocated National Fiber Optic Engineers Conference*, 2010.